Extremum seeking control for optimization of an open-loop grinding mill using grind curves

L. Ziolkowski[a], J. D. le Roux[a], I. K. Craig[a,*]

[a] *Department of Electrical, Electronic and Computer Engineering, University of Pretoria, Pretoria, South Africa.*

Abstract

A semi-autogenous grinding mill is simulated with gradient and non-gradient based extremum seeking controllers to maximize the mill performance using grind curves. Grind curves map the essential performance measures of a grinding mill to the mill load and rotational speed. The curves vary with the changes in the feed ore characteristic but show generic parabolic features with extremums. The extremum seeking controllers search along the unknown input-output map to steer the process towards an unknown optimum. In this study, a classical perturbation-based method, a time-varying parameter estimation-based method and the Nelder-Mead simplex method are employed as extremum seeking control (ESC) methods to search along the grind curves to either optimize the mill throughput or grind by means of manipulating the mill feed or rotational speed. The proposed extremum seeking controller could reduce the need for a plant operator to manually select the optimal operating conditions that maximize the performance measures of a grinding mill. Since the controller is agnostic to the process model, the grinding mill can be optimised without the need for a detailed process model. The simulated results show that the extremum seeking controllers steer the mill operating conditions toward the steady-state optimum and can be used to satisfy operational objectives. However, the slow grinding mill dynamics result in a long convergence rate when the initial conditions are far from the optimal operating conditions.

Keywords: comminution, extremum seeking control, grind curves, grinding mill, modelling, process control, simulation

1. Introduction

Mineral processing consists of several operations to liberate and concentrate the valuable minerals within ore material for further metallurgical extraction processes to produce a useable product. Comminution is the primary stage within a mineral processing plant where the larger run-of-mine ore material is reduced to fine particles through crushing or grinding to liberate the valuable minerals within the ore. The comminution stage plays an important role as the product quality influences the effectiveness of the subsequent downstream operations, and hence the economic value of the concentrate product that is sold to a smelter [1–3].

Consistent product quality from the grinding mill is desired to achieve effective separation in downstream processes to produce a high grade concentrate and minimize the valuable minerals that are lost to the tailings. Therefore, the ore material must be sufficiently ground to a specific particle size, while also maximizing the rate at which the ore is processed. Over-grinding produces a product that may be too fine for separation, a decrease in throughput and an increase in energy consumption. However, the throughput can be increased at the expense of the product quality due to the decreased ore breakage inside the mill. Consequently, this results in a reduced recovery rate at the separation processes. A poor recovery rate, increased energy consumption or decreased throughput contribute to diminishing economic gains [4]. An inverse relationship exists between the throughput and the grind quality and a trade-off has to be considered between the interrelated operational objectives: improve the grind quality, maximize the throughput, and decrease the power consumption to maximize profit [5].

In run-of-mine mineral processing plants, the feed ore composition is regularly changing and the feed ore characteristics such as hardness of the ore and size distribution vary [6, 7]. For semi-autogenous grinding (SAG) mills the grinding media is made up of feed ore and steel balls. Changes in the feed ore characteristics affect the breakage rate of the ore which influences the performance of the grinding mill [8]. Grinding mill circuits are challenging to operate manually and to run at optimal operating conditions due to the complex process behaviour, various unknown disturbances, and strongly-coupled variables [9]. Therefore, manually ensuring that the process is operating at suitable operating conditions to maximize the economic gain would require extensive knowledge of process behaviour and frequent monitoring to compensate for disturbances. In mineral processing plants, a significant

*Corresponding author. Address: Department of Electrical, Electronic, and Computer Engineering, University of Pretoria, Pretoria, South Africa. Tel.: +27 12 420 2172; Fax: +27 12 362 5000. E-mail: ian.craig@up.ac.za

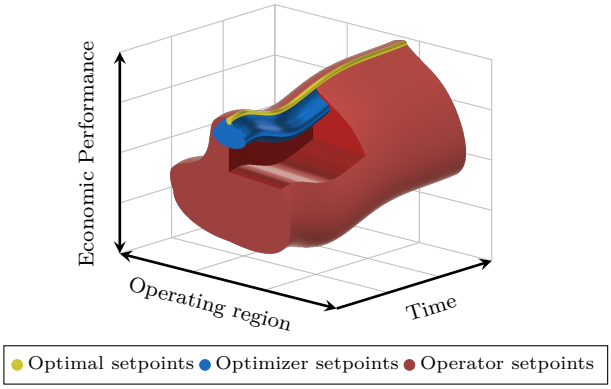

Fig. 1: Economic performance of a grinding mill as a function of the operating conditions.

source of economic loss is typically attributed to poorly chosen operating conditions and further losses are due to the deviations from the chosen operating conditions [10].

In the absence of an optimising controller, the plant operator is responsible for choosing suitable operating conditions for the grinding mill. Insufficient knowledge of the process behaviour in addition to the unknown time-varying factors such as the feed ore variation can lead to sub-optimal operation of the grinding mill.

Two surveys published in 2009 and 2017 [5, 11], highlight the necessity to push for automation within the mineral processing industry. About 30% of the respondents indicated that an operator action occurs at least every 10 minutes and about 20% indicated that the operators are constantly busy ensuring a safely run and profitable operation [11]. The majority of the operator actions (∼50%) being made are changes in the process operating conditions. Therefore, there is an incentive to employ an adaptive real-time optimization controller. The controller would ensure that the process is tracking the optimal operating conditions while satisfying the operational objectives. The optimizer would ideally operate in a region nearer to the optimal operating region compared to the periodic setpoint choices of a plant operator as illustrated in Fig. 1.

Adaptive control can be separated into model-based, partially model-based or model-free methods and is useful in applications where there are variations in process dynamics, parameter uncertainties, disturbances or to improve and optimize processes [12, 13]. The advantage of adaptive control is that the controller is able to utilize online measurements as feedback to directly manipulate process variables to compensate for unknown parameters or disturbances.

Model-based methods are efficient for optimization as the information of the plant behaviour is exploited and used to maximize the performance of the controller to achieve good transient performance. However, developing an accurate model for the complex, non-linear behaviour of a grinding mill is difficult and time-consuming, and requires plant data for validation. Furthermore, for model-based optimization where plant-model mismatch exists, the optimal inputs are only optimal for the model and not necessarily the process itself.

In contrast, model-free adaptive control methods do not use any explicit knowledge of the process dynamics. The method is entirely data-driven based on online measurements from the process. The process is governed by an adaptive update control law that steers the process to optimize an objective function. However, the lack of knowledge of the process behaviour suggests that model-free methods are perhaps better suited for use as optimization controllers that compensate for slowly varying process parameters.

In this paper, model-free adaptive control methods are used to optimize grinding mill performance and are referred to as extremum seeking methods. Extremum seeking control (ESC) is a class of adaptive control techniques used to search for the unknown optimal inputs of a process to maximize (or minimize) an objective function through available measurements. Many extremum seeking methods have been proposed to optimize processes such as perturbation-based ESC [14], sliding mode ESC [15–17], Newton-based ESC [18, 19], numerical optimization ESC [20], estimation-based ESC [21], proportional-integral (PI) ESC [22] and least-squares ESC [23, 24] are just some examples of the development of extremum seeking techniques over the years. The advancement of the ESC techniques aims to improve upon the challenges associated with model-free methods such as the slow convergence rate to the optimum. The application of ESC has extended to various industrial fields such as automotive applications, process control, controller design and optimization, and energy conversion [20]. Examples of extremum seeking applied to optimize grinding circuits in the mineral processing industry are illustrated in [25–27].

A perturbation-based ESC being used on an input-constrained closed grinding mill circuit is illustrated in [25]. The work considers both the problems associated with regulation for setpoint tracking and throughput optimization by maximizing the feed rate of ore material, and also proves the stability of multivariable ESC. Other implementations of extremum seeking techniques, referred to as peak seeking methods have also been employed to optimize grinding circuit performance [26, 27]. The idea is based on the assumption that the maximum throughput of a grinding mill is achieved at maximum power consumption [26]. Therefore, the throughput is maximized with a peak-seeking optimizer to manipulate the mill load filling up to the point where the grinding mill operates at maximum power consumption. However, as later observed in [27], the maximum throughput of the mill is generally achieved below the peak power consumption. The authors of [27] implemented an improved peak-seeking algorithm on a grinding circuit which drives the mill load filling to a point before the peak power consumption and the mill operates closer to the throughput peak.

Grind curves are useful for ESC as they establish the relationships that are observed between the throughput, grind, and power consumption of a mill to the mill filling and rotational speed. Grind curves furthermore indicate where the extremum exists for these performance variables and are parabolic [28–30]. The significance of grind curves is well understood in industry, but their use as part of an ESC strategy is yet to be formalized. A suitable ESC framework can be developed for a general grinding mill circuit that can allow for the optimization of operational objectives, such as maximizing the throughput or grind quality. It would not be necessary to develop explicit grind curves for the mill as the ESC strategy is model-free and only relies on the fact that an extremum exists.

Following the control framework for a grinding circuit presented in [4], a typical process control system would consist of an economic optimizer operating at the highest level, followed by a supervisory control layer and lastly, a regulatory control layer. The need for developing the optimization control layer is indicated by the lack of advanced control technologies implemented in industry [11]. Most processing plants primarily use proportional-integral-derivative (PID) control (∼90%) and less than 40% of the plants have expanded to implementing advanced control methods, such as model predictive control (MPC) [11]. A significant amount of research for controlling grinding circuits is specifically focused on using MPC as a supervisory controller [31–35]. There is however limited research that addresses the development of the optimization control layer [9]. An ESC could operate at the optimization layer and steer the process variables such as the mill filling or speed towards a neighbourhood of the steady-state optimum. These operating conditions are currently mostly set manually.

The contribution of this paper is to demonstrate the value of grind curves combined with ESC as a means to optimize the performance of a grinding mill. For mineral processing plants that do not use a relatively consistent stockpile of ore material, the optimum is time-varying due to feed ore variation. Continuously optimizing the throughput, grind or both can be achieved with ESC by directly using the manipulated variables related to the performance indicators of grind curves.

This paper differs from the optimization strategy described in [26] and [27] where the optimizer uses the power consumption measurements and manipulation of mill load to indirectly maximize throughput. However, this strategy does not guarantee that the optimal throughput is achieved when the mill speed varies. For different mill speeds, the difference between the peak power consumption and throughput does not vary linearly with the mill load [30]. Therefore, tracking the maximum throughput based on power consumption measurements can result in sub-optimal operating conditions if both the mill load and speed is manipulated as is done in this paper. In contrast, [25–27] only use the mill load as a manipulated variable to optimize the mill performance.

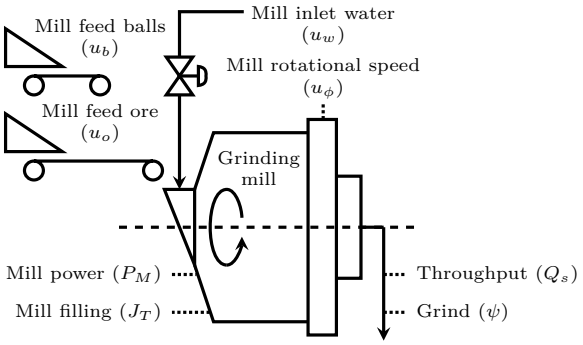

Fig. 2: A semi-autogenous (SAG) mill.

The paper explores several ESC optimization strategies using either the mill load, mill rotational speed or both, as single-input and multiple-input cases, to maximize the throughput, grind or a combination of the two with a weighted objective function. Three extremum seeking optimization methods are considered: a classical perturbation-based method and a time-varying parameter estimation method, which are gradient-based, and a non-gradient based Nelder-Mead simplex method.

The paper is structured as follows. The grinding process is described in Section 2, grind curves are discussed in Section 3, and the process model used to simulate the plant is shown in Section 4. The extremum seeking methods are presented in Section 5. Section 6 demonstrates the application of ESC with simulated results of several optimization scenarios. The paper is concluded in Section 7.

2. Process description

A SAG mill is illustrated in Fig. 2. The nomenclature is shown in Table 1. The mill receives three streams: mined ore (u_o), water (u_w), and steel balls (u_b). The mill charge is a mixture of grinding media and slurry. Grinding media refers to the steel balls and rocks which break the ore and slurry refers to the mixture of solids and water. The fraction of the mill filled with charge is denoted by J_T.

Table 1: Description of comminution circuit variables.

Variable	Unit	Description
J_T	[-]	Fraction of mill volume filled with charge
P_M	[kW]	Mill power draw
Q_w	[m^3/h]	Water discharge flow rate
Q_s	[m^3/h]	Solids discharge flow rate
Q_f	[m^3/h]	Fines discharge flow rate
ρ_o	[t/m^3]	Ore density
ψ	[-]	Grind (volume fraction of particles in discharge < 150 μm)
u_b	[t/h]	Feed rate of steel balls
u_o	[t/h]	Feed rate of ore
u_w	[m^3/h]	Flow rate of feed water
u_ϕ	[-]	Fraction of critical mill speed

Grinding mills rotate along their longitudinal axis and the rotational speed is expressed as a fraction of the critical mill speed (u_ϕ). The critical mill speed is defined as the rotational speed where the centrifugal forces acting on the mill charge particles is equal to the gravitational force. Therefore, at the critical mill speed the mill charge travels along the mill shell, instead of cascading inside the mill. At sub-critical mill speeds, the rotating shell of the mill creates a cascading motion of charge inside the mill which causes the ore to break through impact breakage, abrasion, and attrition. The ground ore in the mill mixes with water to create a slurry which discharges through an end-discharge grate. Ore too large to pass through the end-discharge grate are referred to as *rocks* and must be broken further. All ore small enough to pass through the end-discharge grate are referred to as *solids*. The flow rate of solids and water discharging from the mill is given by Q_s and Q_w respectively. Q_s is the volumetric throughput of solids through the mill and is equal to u_o/ρ_o at steady-state where ρ_o is the ore density.

The aim of the grinding mill is to grind the ore to below a specification size, e.g., 150 μm. The mill grind (ψ) is the volume fraction of material in the discharge of the mill below the specification size. The broken ore below the specification size is referred to as *fines*. Note, whereas solids refer to all ore small enough to discharge from the mill, fines refer to the portion of solids smaller than the specification size. The discharge flow rate of fines from the mill is given by Q_f.

Grinding mills are typically operated to maximize Q_s while keeping the grind particle size within an acceptable range. The net revenue generated from an increased throughput is often perceived to exceed the economic value that could be generated from the losses incurred in the separation process due to the decreased grind quality. However, depending on the market and ore availability it could be beneficial to maintain a set throughput and minimize the product particle size variation to increase recovery rates [4, 36, 37]. The mill charge is primarily controlled to achieve the desired throughput by manipulating u_o and u_w. However, in situations where the feed ore hardness or size varies and the mill charge cannot be effectively controlled to compensate for the disturbances, manipulating u_ϕ adds an additional degree of freedom to control Q_s or ψ [34, 38].

3. Grind curves

The performance indicators of a grinding mill are throughput (Q_s), grind (ψ) and power consumption (P_M). Grind curves describe the relationships between these performance indicators as a function of the mill filling (J_T) and mill speed (u_ϕ) [29]. A notable characteristic of grind curves is that they are parabolic and indicate the peaks of the performance indicators as the mill load is varied for different constant mill speeds. Importantly, as the feed ore characteristics such as hardness vary, the peaks of the performance indicators shift while the parabolic trend is preserved for different ore types [28, 39]. Grind curves can be used to [29]:

- act as reference for operating the grinding circuit when the feed ore characteristics vary,
- identify the optimum mill filling for a given mill rotational speed to meet the operational objectives for throughput or grind, and
- operate the mill at a stable region.

The issue with using grind curves as a reference for operating the mill are twofold. Firstly, manually operating the grinding mill based on grind curves would require that for each ore type there is already a set of grind curves that have been established. The grind curves are obtained by progressively stepping through a range of operating conditions and allowing the mill to reach steady-state for each step. This is a costly and time-consuming task [30]. Secondly, if the feed ore characteristic varies, the operator would have to be aware of the change and make the necessary changes to ensure that the mill is operating at the new optimum. Therefore, it can be beneficial if an adaptive control system is implemented that searches along the grind curves in real-time to locate the unknown peak. Therefore, such a control system would implicitly use the knowledge that grind curves are parabolic to steer the grinding mill toward an optimum.

Grind curve data from an industrial mill is presented in [29]. The peaks of the grind curves in [29] are provided in Table 2 and are used to fit the performance indicators as quadratic polynomials in terms of J_T for each u_ϕ. Subsequently, the performance indicators are fit as cubic polynomials in terms of u_ϕ [34].

Fig. 3 illustrates the grind curves of [29] and indicates where the curves are extrapolated outside the measured range of the industrial mill. The 3-D surface maps of the grind curves in Fig. 3 are shown Fig. 4. Interestingly, the optimum Q_s and ψ occur at similar values of J_T when $u_\phi = 0.75$. However, this is not the case for lower values of u_ϕ. The surface maps of the grind curves clearly indicates the trade-off that has to be made when optimizing either Q_s or ψ. Assuming that J_T is kept constant, an increase in Q_s can be achieved by increasing u_ϕ at the cost of a decrease in ψ, and vice-versa. Alternatively, by maintaining u_ϕ constant, Q_s is maximized by increasing J_T up to an extreme after which Q_s begins to decrease. If

Table 2: Performance indicator peaks from [29] as illustrated in Fig. 3.

Mill speed	Throughput		Grind		Power	
u_ϕ[-]	J_T [-]	Q_s [m^3/h]	J_T [-]	ψ [-]	J_T [-]	P_M [kW]
0.75	0.35	157.0	0.33	0.56	0.39	4037
0.70	0.31	120.7	0.37	0.69	0.47	4028
0.65	0.23	93.3	0.58	0.94	0.55	3931
0.60	0.18	96.7	0.63	1.00	0.54	3603

the mill charge begins to accumulate, less breakage occurs and Q_s is reduced. Maximizing ψ is usually not as beneficial as there is a maximum acceptable grind quality after which the product is too fine for the separation process to perform optimally [4]. In addition, because over-grinding wastes energy, it is common for the operational objectives of a grinding mill circuit to maximize Q_s until the minimum acceptable ψ is achieved. The acceptable grind size is usually chosen based on the grain size of the valuable minerals which minimizes the grinding effort required to liberate the minerals from the gangue [1].

4. Grinding mill

The SAG mill in Fig. 2 is described with a dynamic non-linear model [40]. The model is fit to the grind curve data from [29] using the step-wise procedure described in [41]. The model produces a realistic dynamic and steady-state response over a wide range of operating conditions which is suitable for testing an extremum seeking controller in search of an unknown optimum. In other words, ESC is agnostic to the simulation model of the plant. A brief overview of the simulation model in [41] is presented here.

4.1. Model description

The state-space description of the model is,

$$\dot{\mathbf{x}} = \mathbf{f}(t, \mathbf{x}, \mathbf{u}), \tag{1a}$$
$$\mathbf{y} = \mathbf{h}(t, \mathbf{x}, \mathbf{u}), \tag{1b}$$

where the state vector is $\mathbf{x} = [x_w,\ x_s,\ x_r,\ x_f]^T$, the input vector is $\mathbf{u} = [u_w,\ u_o,\ u_\phi]^T$, and the output vector is $\mathbf{y} = [J_T,\ P_M,\ Q_s,\ \psi,\ \beta_{ws}]^T$. The state equations are,

$$\dot{x}_w = u_w - Q_w, \tag{2a}$$
$$\dot{x}_s = (1-\alpha_r)\frac{u_o}{\rho_o} - Q_s + Q_{rc}, \tag{2b}$$
$$\dot{x}_r = \alpha_r \frac{u_o}{\rho_o} - Q_{rc}, \tag{2c}$$
$$\dot{x}_f = \alpha_f \frac{u_o}{\rho_o} - Q_f + Q_{fp}, \tag{2d}$$

where x_w, x_s, x_r and x_f represent the volume of water, solids, rocks, and fines in the grinding mill respectively, α_f is the fraction of fines in u_o, and α_r is the fraction of rocks in u_o. Q_{rc} is the rock consumption and Q_{fp} is the fines produced which is defined in (11a) and (11b) respectively. The grinding mill discharge flow rates are defined as,

$$Q_w = d_q x_w \varphi\left(\frac{x_w}{x_s + x_w}\right), \tag{3a}$$
$$Q_s = d_q x_w \varphi\left(\frac{x_s}{x_s + x_w}\right), \tag{3b}$$
$$Q_f = d_q x_w \varphi\left(\frac{x_f}{x_s + x_w}\right), \tag{3c}$$

where d_q is the discharge rate constant. The volume of the water to solids ratio in the discharged slurry is denoted by β_{ws}. It is used in [41] in a feedback loop to maintain a constant slurry density and from (3a) and (3b) it is equivalent to,

$$\beta_{ws} = \frac{Q_w}{Q_s}. \tag{4}$$

A ratio equal to $\beta_{ws} = 1.5$ indicates that the slurry consists only of water and if $\beta_{ws} = 0$, the slurry is a non-flowing mud. The grind of the mill is defined as a ratio of the discharged flow rate of the fines to the solids,

$$\psi = \frac{Q_f}{Q_s}. \tag{5}$$

The fraction of the total mill filled with charge is,

$$J_T = \frac{x_w + x_s + x_r + x_b}{V_{mill}}, \tag{6}$$

where x_b is the volume of steels balls in the mill and V_{mill} is the total internal volume of the mill. The mill power consumption is modelled as a function of J_T and u_ϕ,

$$\begin{aligned} P_M(J_T, u_\phi) =& P_{max}(u_\phi)\left(1 - \delta_s\left(\frac{\varphi}{\varphi_N} - 1\right)^2\right) \\ & - P_{max}(u_\phi)\left(\delta_v\left(\frac{J_T}{J_{T,P_{max}}(u_\phi)} - 1\right)^2\right) \end{aligned} \tag{7}$$

where δ_v and δ_s is the power change parameter for the volume of mill filled and for the volume fraction of solids in the slurry respectively, φ is the rheology factor, and φ_N is the normalization factor. $J_{T,P_{max}}(u_\phi)$ is a parameterized function of the fraction of the mill filled at maximum power draw given by,

$$J_{T,P_{max}}(u_\phi) = -7.52u_\phi^2 + 9.06u_\phi - 2.18, \tag{8}$$

and $P_{max}(u_\phi)$ [kW] is a parameterized function of the maximum mill power consumption given by,

$$P_{max}(u_\phi) = \left(-2.70u_\phi^2 + 3.92u_\phi - 1.02\right) \times 10^4. \tag{9}$$

The empirical rheology factor (φ) is given by,

$$\varphi = \begin{cases} \sqrt{1 - \frac{x_s}{x_w}\left(\epsilon_0^{-1} - 1\right)} & , \text{ if } \frac{x_s}{x_w} \leq \left(\epsilon_0^{-1} - 1\right)^{-1} \\ 0 & , \text{ if } \frac{x_s}{x_w} > \left(\epsilon_0^{-1} - 1\right)^{-1} \end{cases} \tag{10}$$

where ϵ_0 is the maximum fraction of solids by volume of slurry at zero slurry flow.

The grinding operation consumes grinding media, resulting in the production of fine and solid particles. The ball filling (x_b) is assumed to be kept constant during the grinding operation. The rock consumption (Q_{rc}) and fines produced (Q_{fp}) functions are defined as,

$$Q_{rc} = \frac{P_M(J_T, u_\phi)}{\rho_o K_{rc}(J_T, u_\phi) \times 10^6}, \tag{11a}$$

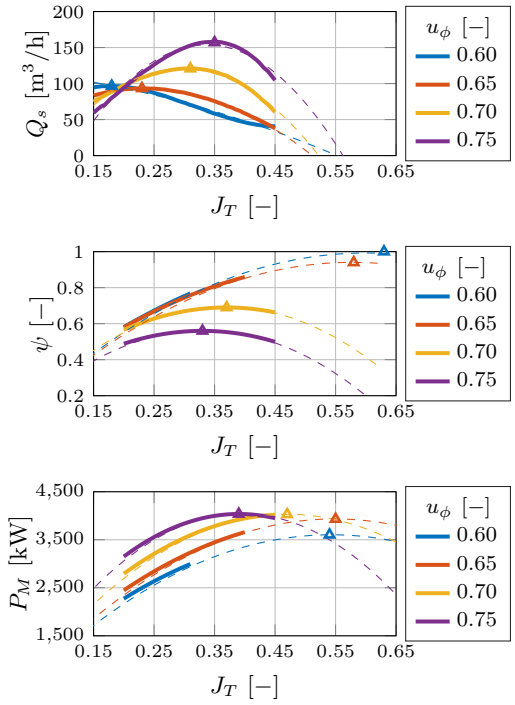

Fig. 3: Grind curves for throughput (Q_s), grind (ψ), and power (P_M) reproduced from [29]. The dashed lines show the extrapolated curves and the △ data markers indicate the peaks for each value of u_ϕ.

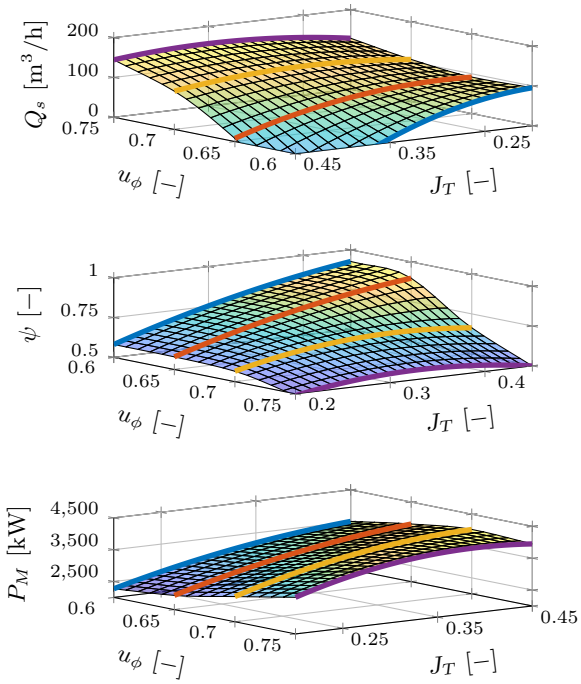

Fig. 4: Grind curve surface maps for throughput (Q_s), grind (ψ), and power (P_M) shown in Fig. 3 as reproduced from [29].

$$Q_{fp} = \frac{P_M(J_T, u_\phi)}{\rho_o K_{fp}(J_T, u_\phi) \times 10^6}, \tag{11b}$$

where the factors K_{rc} and K_{fp} are functions which indicate the energy required per tonne of rocks consumed and fines produced respectively,

$$\begin{aligned} &K_{rc}(J_T, u_\phi) = \\ &(-0.478u_\phi^3 - 3.06u_\phi^2 + 1.55u_\phi - 0.183)J_T^3 \\ &+(2.68u_\phi^3 + 5.13u_\phi^2 - 2.92u_\phi + 0.355)J_T^2 \\ &+(-3.15u_\phi^3 - 2.61u_\phi^2 + 1.78u_\phi - 0.226)J_T \\ &+(1.05u_\phi^3 + 0.361u_\phi^2 - 0.352u_\phi + 0.047), \end{aligned} \tag{12a}$$

$$\begin{aligned} &K_{fp}(J_T, u_\phi) = \\ &(-3.73u_\phi^3 + 0.602u_\phi^2 + 0.301u_\phi - 0.049)J_T^3 \\ &+(8.76u_\phi^3 - 1.97u_\phi^2 - 0.453u_\phi + 0.088)J_T^2 \\ &+(-6.82u_\phi^3 + 1.91u_\phi^2 + 0.180u_\phi - 0.05)J_T \\ &+(1.77u_\phi^3 - 0.581u_\phi^2 - 0.007u_\phi + 0.009). \end{aligned} \tag{12b}$$

4.2. Model simulation

4.2.1. Dynamics response

A step response of the plant (Fig. 5) is shown in Fig. 6 to demonstrate the plant dynamics and the interactions between the performance indicators, throughput (Q_s) and grind (ψ), and the manipulated variables, mill load setpoint ($J_{T,sp}$) and mill speed (u_ϕ). The mill load (J_T) is controlled to setpoint ($J_{T,sp}$) with a PI controller by manipulating the feed ore (u_o). Another PI-controller is used to regulate the water to solids ratio at $\beta_{ws,sp} = 0.9$ by manipulating the inlet water (u_w) to ensure a constant slurry density so that the discharge slurry from the mill is a flowing mixture. The dynamics associated with Q_s and ψ are relatively slow, the process reaches steady-state after approximately 2 hours when $J_{T,sp}$ or u_ϕ is stepped. An increase in J_T increases both Q_s and ψ, whereas decreasing u_ϕ shows a decrease in Q_s and an increase in ψ.

4.2.2. Steady-state response

The steady-state step response of the model is shown in Fig. 7. The 3-D surface maps of Q_s, ψ and P_M are obtained by sweeping the model over the range $J_T \in [0.20, 0.45]$ and $u_\phi \in [0.60, 0.75]$ starting from

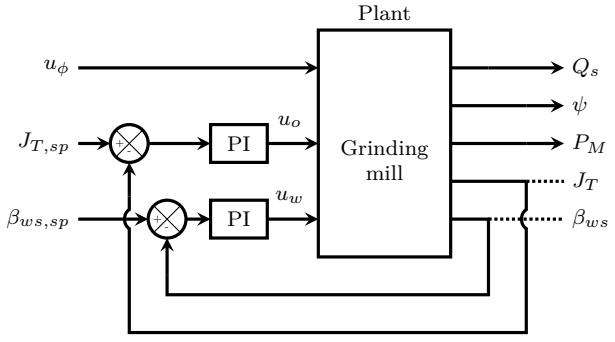

Fig. 5: Block diagram of the feedback control loops of the grinding mill.

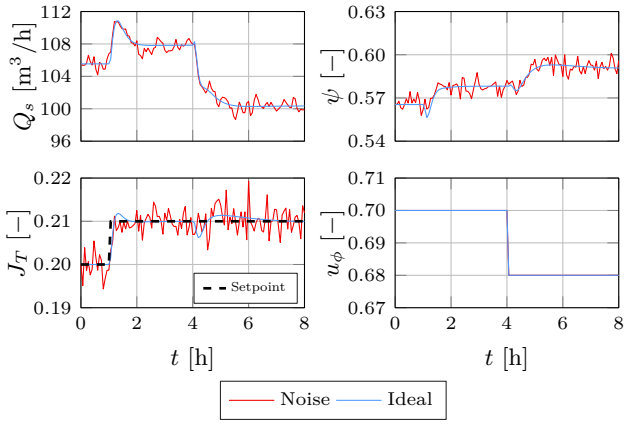

Fig. 6: Plant step response with and without additive white Gaussian measurement noise. The mill load setpoint ($J_{T,sp}$) is stepped at $t = 1$ h and the mill speed (u_ϕ) is stepped at $t = 4$ h.

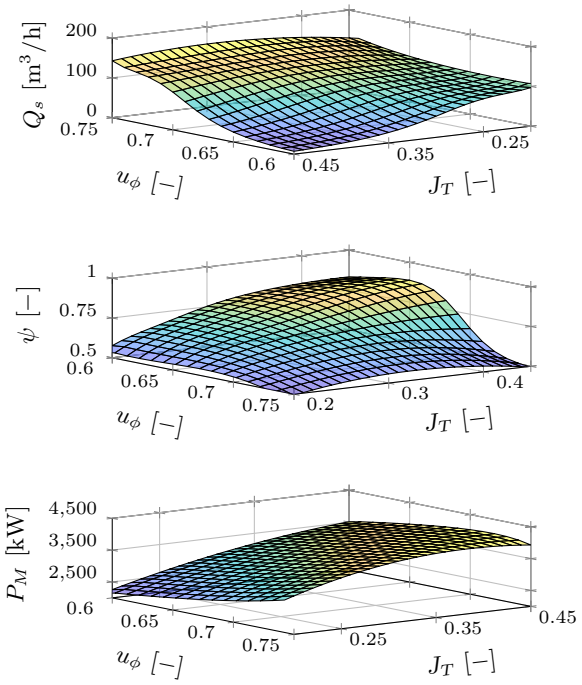

Fig. 7: 3-D surface map of the steady-state plant model response.

$(J_T, u_\phi) = (0.20, 0.75)$.

The grind curves in Fig. 4 measured at the industrial circuit compare well to the simulated grind curves in Fig. 7. There is a good correlation in the maps for Q_s and P_M. However, because the model extrapolates the peak positions for ψ at low u_ϕ past the observed industrial grind curve data, the surface map of the modelled ψ in Fig. 7 differs slightly from the surface map for ψ in Fig. 4.

5. Extremum seeking control (ESC)

Extremum seeking control (ESC) is an optimization technique that maximizes an objective function by exploring an unknown static map and steering the system towards the optimal operating condition. The motive behind choosing an extremum seeking method is based on either the ease of tuning or the desired optimization performance. A controller with more tuning parameters can be more difficult to tune, but it is more likely to achieve the desired performance. The performance indicators of an extremum-seeking controller to consider are [42],

- **Speed of convergence:** the convergence rate at which the optimization method evolves toward an extremum.
- **Domain of convergence:** the region of attraction toward an extremum. A larger domain of convergence is likely to converge toward a global extremum, whereas a smaller domain of convergence is likely to converge toward a local extremum.
- **Accuracy:** the size of the neighbourhood to which the optimized variable converges to.

5.1. Perturbation-based extremum seeking (PESC)

Perturbation-based extremum seeking (PESC) is a gradient-search method that is dependent on a measurable, convex objective function and does not rely on the explicit knowledge of the process behaviour. PESC employs a periodic excitation or dither signal added to the input of the system, which is used to obtain the gradient information of the objective function. The PESC scheme is shown in Fig. 8 and the closed-loop system dynamics with ESC are described by [14],

$$\dot{x} = f(t, x, \theta), \tag{13a}$$
$$y = h(t, x, \theta), \tag{13b}$$
$$\dot{\hat{\theta}} = k\xi, \tag{13c}$$
$$\dot{\xi} = -\omega_l \xi + \omega_l (y - \eta) a \sin(\omega t), \tag{13d}$$
$$\dot{\eta} = -\omega_h \eta + \omega_h y, \tag{13e}$$

where the unknown process dynamics are described by $\dot{x}$, y is the measurable output, and, ω_l and ω_h are the cut-off frequencies for the low-pass and high-pass filters respectively. The state of the high-pass filter is indicated

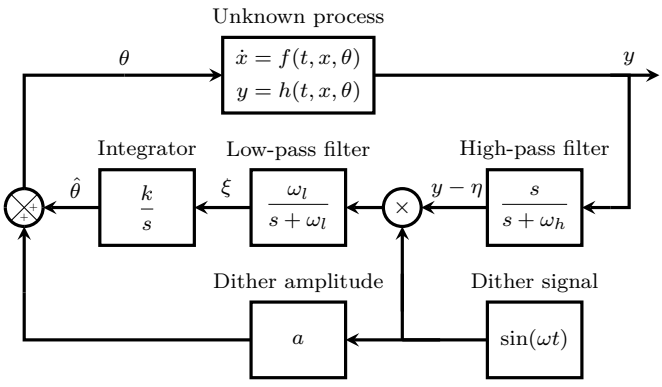

Fig. 8: Perturbation-based extremum seeking scheme [14].

by η which removes the DC component or average value from the perturbed output, resulting in the filtered output, $y - \eta$. A low-pass filter is used to reduce the effects of high-frequency noise and the estimated gradient (ξ) is driven to zero by an integrator with gain, k. The best estimate of the optimal input ($\hat{\theta}$) converges towards the unknown optimal input. The input (θ) to the process consists of the best estimate of the optimal input ($\hat{\theta}$) and the periodic dither signal,

$$\theta = \hat{\theta} + a\sin(\omega t), \tag{14}$$

where a and ω is the dither amplitude and frequency respectively.

Applying extremum seeking to a dynamic process requires a sufficient time-scale separation between the perturbation frequency and the process dynamics to enable the optimizer to search through an unknown static map [14]. Therefore, it is required that a suitable perturbation frequency is chosen such that the process dynamics operate at the fastest time-scale, followed by the medium time-scale dynamics of the perturbation signal, and finally the slowest time-scale for the optimization. A slow perturbation signal is necessary to avoid the process dynamics from interfering with the estimation of the gradient. Therefore, the input-output relationship of the process can be viewed as a static plant. For the case of multiple-input, single-output systems, additional time scale separations are required to separate the effects of each input. Consequently, the range of ω for each input is further limited. Further, the cut-off frequency of the high-pass and low-pass filter should be lower than the chosen perturbation frequency, and k needs to be chosen to be sufficiently small. The amplitude for the dither signal should be chosen to be larger than the expected noise, but small enough to minimize the perturbations that propagate to the output, such that ESC converges to a sufficiently small neighbourhood of the optimum. Due to the required time-scale separations necessary for convergence, PESC has transient performance limitations that are related to the dynamics of the process.

5.2. Time-varying parameter estimation extremum seeking (TESC)

The time-varying parameter estimation extremum seeking control (TESC) method proposed in [21] is based on estimating the gradient as a time-varying parameter. The method optimizes an objective function by estimating the unknown time-varying parameter $\hat{\theta}$, which minimizes the objective function. Similar to the perturbation-based method, a dither signal is required to excite the system and extract gradient information. However, the advantage of TESC is that it provides additional freedom in tuning the controller, which can achieve improved transient performance. As opposed to PESC, the tuning of the controller is not primarily limited to the tuning parameters of the dither signal. The TESC scheme is shown in Fig. 9

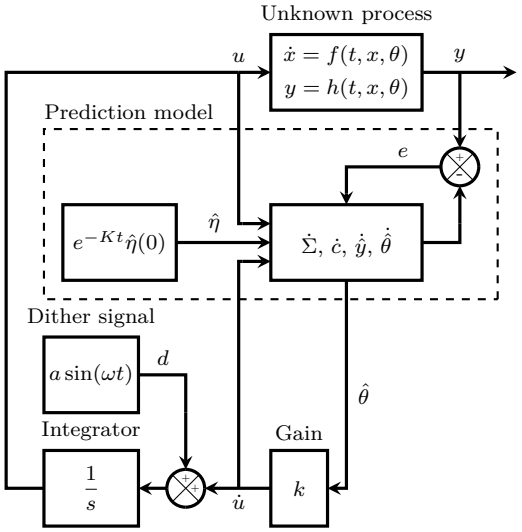

Fig. 9: Time-varying parameter estimation extremum seeking scheme (adapted from [43]).

and the closed-loop system dynamics are given by,

$$\dot{x} = f(t,x,u), \tag{15a}$$
$$y = h(t,x,u), \tag{15b}$$
$$K = k_{\eta_1} + k_{\eta_2} c^T c, \tag{15c}$$
$$\dot{u} = -k\hat{\theta} + d, \tag{15d}$$
$$\dot{\hat{\theta}} = \mathrm{Proj}\Big\{\Sigma^{-1}(c(e-\hat{\eta}) - \sigma\hat{\theta}), \hat{\theta}\Big\}, \tag{15e}$$
$$\dot{\hat{y}} = \dot{u}^T\hat{\theta} + Ke + c^T\dot{\hat{\theta}}, \tag{15f}$$
$$\dot{c} = -Kc + \dot{u}, \tag{15g}$$
$$\dot{\hat{\eta}} = -K\hat{\eta}, \tag{15h}$$
$$\dot{\Sigma}^{-1} = -\Sigma^{-1}cc^T\Sigma^{-1} + k_T\Sigma^{-1} - 2\sigma\Sigma^{-2}, \tag{15i}$$

where $e = y - \hat{y}$, is the error between the measured and predicted output, $d = \alpha\sin(\omega t)$ is the dither signal, K is a time-varying gain, and $\hat{\eta}$ is the estimation error. The combination of $\hat{y}$, c, $\hat{\eta}$ and Σ form the prediction model for estimating the unknown time-varying parameter. The projection operator, $\mathrm{Proj}\Big\{\phi, \hat{\theta}\Big\}$ is defined as,

$$\dot{\hat{\theta}} = \begin{cases} \phi, & \text{if } \mathcal{P}(\hat{\theta}) > 0 \text{ or } \nabla_{\hat{\theta}}\mathcal{P}(\hat{\theta})\phi \leq 0 \\ \left(I - \frac{\nabla_{\hat{\theta}}\mathcal{P}(\hat{\theta})^T\nabla_{\hat{\theta}}\mathcal{P}(\hat{\theta})}{\|\nabla_{\hat{\theta}}\mathcal{P}(\hat{\theta})\|^2}\right)\phi, & \text{otherwise,} \end{cases} \tag{16}$$

where $\phi = \Sigma^{-1}(c(e-\hat{\eta}) - \sigma\hat{\theta})$ and the function $\mathcal{P}(\hat{\theta})$ is defined as,

$$\mathcal{P}(\hat{\theta}) = ||\hat{\theta}||^2 - z_{\hat{\theta}}^2, \tag{17}$$

where $z_{\hat{\theta}}$ is the radius of the uncertainty set. The gradient of $\mathcal{P}(\hat{\theta})$ is given by,

$$\nabla_{\hat{\theta}}\mathcal{P}(\hat{\theta}) = 2\hat{\theta}^T. \tag{18}$$

The projection operator is used to limit the transients of the parameter estimate within defined bounds and it

guarantees that the unknown parameter is within the uncertainty set $\hat{\theta} \in \Pi$, $\forall t > 0$, providing robustness to the prediction model. Therefore, the unknown parameter converges towards its true estimate value within the set boundary. K and k_T are the optimization estimation gains, and, k_{η_1} and k_{η_2} are positive constants to be assigned [21]. The optimization gain affects the speed of the optimization, but it cannot be arbitrarily increased. An increased gain reduces the effects of the dither signal, which in turn affects the estimation routine. If k is chosen too large, it can result in an oscillatory behaviour as the speed of the process dynamics become negligible relative to the ESC dynamics. The tuning parameter, σ, should be chosen as small as possible to guarantee that the parameter estimation routine can effectively track the time-varying gradient. The purpose of σ is to ensure that Σ does not become too small which would impede the estimation routine. Finally, z_θ has to increase for smaller choices of σ [43].

5.3. Simplex extremum seeking (SESC)

Simplex extremum seeking control (SESC) is based on the Nelder-Mead simplex algorithm. It is an optimization method that minimizes an objective function without utilizing gradient information [44]. Instead, it is an iterative direct search method that evaluates the function values of an objective function at a set of points to form a simplex. In each iteration the simplex is transformed by means of either four operations: reflection, expansion, contraction about the simplexes centroid or the simplex is shrunk. The coefficients used to influence the effect of each operation should satisfy,

$$\rho > 0,\ \chi > 1,\ 0 < \gamma < 1,\ 0 < \sigma < 1, \tag{19}$$

where ρ, χ, γ and σ are the coefficients of reflection, expansion, contraction and shrinkage, respectively. The Nelder-Mead simplex method is described in Algorithm 1. At each step of the iteration a new vertex is computed and the objective function corresponding to the vertex is evaluated and ranked. An operation that produces a lower objective function value is accepted and the new point replaces the worst performing vertex at the end of the iteration. These operations lead to the vertices of the simplex to converge toward a solution that minimizes the objective function.

The simplex method is applied to optimize a dynamic process by assigning the values of the simplex vertices to the inputs of the process and allowing a sufficient period (T_s) for the process to reach steady-state before manipulating the inputs again. However, depending on the coefficients chosen, this can lead to undesired plant behaviour such as overshooting if a step-size is too large. This is especially important in the case of the grinding mill considered in this paper as it is sensitive to step changes in the mill load or rotational speed [34]. The manipulated variables transition from the previous iteration operating point to the new operating point by interpolating between

Algorithm 1 Nelder-Mead simplex method adapted from [45].

Setup:
$\boldsymbol{\theta}^{(0)} \leftarrow [\theta_1, ..., \theta_n]$ (Initial conditions)
$\rho > 0,\ \ \chi > 1,\ \ 0 < \gamma < 1,\ \ 0 < \sigma < 1$

Initialization:
Form the initial simplex around $\boldsymbol{\theta}^{(0)}$
$$\mathbf{v}_m^{(0)} = \boldsymbol{\theta}^{(0)} + h\mathbf{j}_m,\ m = 1, ..., n+1$$
where $\mathbf{v}_m$ is a vertex of the simplex, h is a step size and $\mathbf{j}$ is a unit vector in the m-th dimension.

Repeat:
Begin iteration, i
Rank the performance at each vertex such that,
$$J(\mathbf{v}_1^{(i)}) < ... < J(\mathbf{v}_n^{(i)}) < J(\mathbf{v}_{n+1}^{(i)})$$
where $\mathbf{v}_1^{(i)}$ is the *best* point and $\mathbf{v}_{n+1}^{(i)}$ is the *worst* point in the set of vertices for the current iteration.

Compute the centroid of the vertices
$$\bar{\mathbf{v}} = \frac{\sum_{k=1}^{n} \mathbf{v}_k^{(i)}}{n}$$
$\mathbf{v}_r = \bar{\mathbf{v}} + \rho(\bar{\mathbf{v}} - \mathbf{v}_{n+1}^{(i)})$ (*reflection*)

if $J(\mathbf{v}_r) < J(\mathbf{v}_1^{(i)})$ **then**
  $\mathbf{v}_e = \mathbf{v}_r + \chi(\mathbf{v}_r - \bar{\mathbf{v}}$ (*expansion*)
  if $J(\mathbf{v}_e < J(\mathbf{v}_r)$ **then**
    $\mathbf{v}_{n+1}^{(i+1)} = \mathbf{v}_e$ (*accept expansion point*)
  else
    $\mathbf{v}_{n+1}^{(i+1)} = \mathbf{v}_r$ (*accept reflection point*)
  end if
else
  if $J(\mathbf{v}_r) < J(\mathbf{v}_n^{(i)})$ **then**
    $\mathbf{v}_{n+1}^{(i+1)} = \mathbf{v}_r$ (*accept reflection point*)
  else
    if $J(\mathbf{v}_r) < J(\mathbf{v}_{n+1}^{(i+1)})$ **then**
      $\mathbf{v}_{co} = \bar{\mathbf{v}} + \gamma(\mathbf{v}_r - \bar{\mathbf{v}}$ (*outside contraction*)
      if $J(\mathbf{v}_{co}) \leq J(\mathbf{v}_r)$ **then**
        $\mathbf{v}_{n+1}^{(i+1)} = \mathbf{v}_{co}$ (*accept outside contraction point*)
      else
        $\mathbf{v}^{(i+1)} = \mathbf{v}_1^{(i)} + \sigma(\mathbf{v}_j^{(i)} - \mathbf{v}_1^{(i)}),\ j = 2, ..., n+1$
        (*shrink*)
      end if
    else
      $\mathbf{v}_{ci} = \bar{\mathbf{v}}^{(i)} - \gamma(\bar{\mathbf{v}} - \mathbf{v}_{n+1}^{(i)})$ (*inside contraction*)
      if $J(\mathbf{v}_{ci}) < J(\mathbf{v}_{n+1}^{(i+1)})$ **then**
        $\mathbf{v}_{n+1}^{(i+1)} = \mathbf{v}_{ci}$ (*accept inside contraction point*)
      else
        $\mathbf{v}^{(i+1)} = \mathbf{v}_1^{(i)} + \sigma(\mathbf{v}_j^{(i)} - \mathbf{v}_1^{(i)}),\ j = 2, ..., n+1$
        (*shrink*)
      end if
    end if
  end if
end if
Terminate iteration

the points through a straight line function that is described by,

$$x(t) = \left(\frac{x_n - x_p}{t_n - t_p}\right)(t - t_p) + x_p, \tag{20}$$

where $x(t)$ is the value of the operating point at time t, x_n and x_p are the new and previous operating points respectively, and t_n and t_p are the start time and end time respectively, for which the ramp transition occurs. This reduces the aggressive plant behaviour during the transient response between steps and produces a response without

Table 3: Model parameter values.

Variable	Value	Description
α_f	0.1 [-]	Fraction of fines in u_o
α_r	0.5 [-]	Fraction of rocks in u_o
ρ_o	2.7 [t/m^3]	Ore density
d_q	36.4 [1/h]	Discharge rate constant
x_b	16.4 [m^3]	Volumetric filling of balls in mill
V_{mill}	208 [m^3]	Total mill volume
δ_v	0.923 [-]	Power change parameter for the volume of mill filled
δ_s	0.923 [-]	Power change parameter for volume fraction of solids in the slurry
φ_N	0.509 [-]	Rheology normalization factor
ϵ_0	0.6 [-]	Maximum fraction of solids by volume of slurry at zero slurry flow

excessive overshoot.

The simplex method only evaluates the objective function itself and not the gradient of the function. Therefore, SESC is robust to the presence of noise or small variations in the objective function. The disadvantage of SESC is that as the method converges toward the optimum the size of the simplex decreases, effectively reducing the magnitude of the perturbations. As the simplex size decreases, the method maintains the operating points at the same conditions. If the optimum then changes the method is unable to react accordingly and adjust the simplex to track the new optimum. Therefore, the method has to be reinitialized to begin tracking the new optimum. The challenge is to identify how often this occurs, while reducing the number of disturbances that occur due to the method attempting to find the new optimum. Therefore, the method is primarily suitable for optimizing a static objective function. Although, it is not considered in this paper, the method can be adapted to implement a fixed or variable simplex size to track a time-varying optimum, referred to as the dynamic simplex method [46]. This is achieved by enforcing a minimum simplex size to ensure that during run time the step size is always sufficiently large to disturb the process and track the optimum.

An additional aspect to consider for SESC is the tuning parameters of the simplex algorithm. For example, if the step size for the mill load is large and the settling time (T_s) is chosen to be sufficiently long, the mill could be unintentionally driven towards an unstable operating condition. For example, if a high mill load setpoint is assigned by the SESC, the mill will begin to overfill and require intervention to be emptied manually to resume operation.

6. Results and discussion

In this section, several strategies demonstrate the application of the ESCs for optimizing grinding mill performance. The parameters used to simulate the model described in (1) to (12) are provided in Table 3. The aim is not to determine the best extremum-seeking method, but rather to evaluate the application of the ESCs for a grinding mill and their ability to converge toward an extremum. To illustrate how the ESC steers the process along the grind curves, the results of the ESC trajectories are projected onto the 3-D surface map of the model response (Fig. 7) for the chosen optimized output.

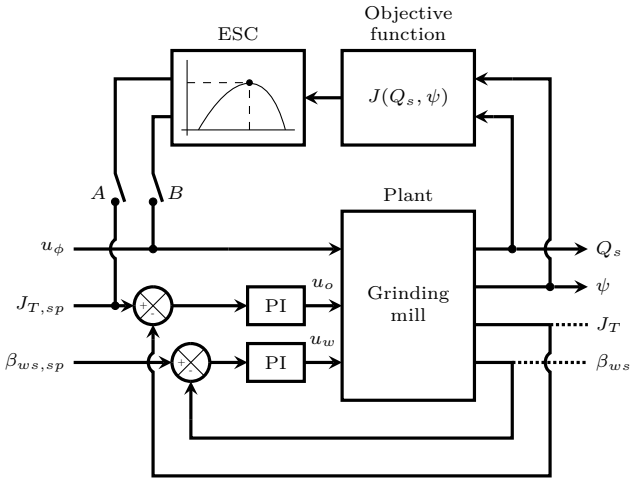

Fig. 10: Block diagram of the grinding mill controlled with ESC.

The configuration of the plant with ESC is illustrated by the block diagram in Fig. 10. The purpose of the ESC objective function is to maximize the measured throughput or grind of the mill,

$$J(Q_s,\ \psi) = Q_s \ \text{(throughput optimization)}, \tag{21a}$$
$$J(Q_s,\ \psi) = \psi \quad \text{(grind optimization)}. \tag{21b}$$

The ESC optimizes the mill performance by manipulating $J_{T,sp}$ or u_ϕ. If the mill load is used, the ESC perturbations are added to $J_{T,sp}$ and the PI-controller aims to track the perturbed setpoint. In comparison, the ESC can directly perturb u_ϕ. The configuration in Fig. 10 illustrates that either $J_{T,sp}$ or u_ϕ can be separately manipulated while the other variable is kept constant, or both can be simultaneously manipulated by the ESC to steer the grinding mill. If either of the manipulated variables are disconnected from the ESC by opening switch A or B in Fig. 10, they are set to a constant value.

There is no formal or systematic approach followed to tune the ESCs to achieve a desired performance criteria. Each of the ESCs were tuned through trial and error to achieve a reasonable balance between the ESC performance indicators discussed in Section 5. Specific attention was paid to achieving good transient performance and convergence speed, taking into consideration the process dynamics.

The performance of the various ESC algorithms is evaluated and compared according to their rate of convergence. The ESC criteria for convergence is chosen as the time it takes for the ESC to reach and settle within a 2% threshold of the final mean value of the objective function. The simulated results are post-processed with a moving average filter with a window size of 10 samples so that the noise

Table 4: SISO throughput (Q_s) ESC tuning parameters.

Method	Manipulated variable	Tuning parameter values	Results
PESC	$J_{T,sp}$	$k = 25$, $a = 0.002$, $\omega_h = 1.8$ rad/h, $\omega = 2$ rad/h, $\omega_l = 0.1$ rad/h	Fig. 11
	u_ϕ	$k = 25$, $a = 0.002$, $\omega_h = 1.8$ rad/h, $\omega = 2$ rad/h, $\omega_l = 0.1$ rad/h	
TESC	$J_{T,sp}$	$k_T = 2$, $k_{\eta_1} = 0.25$, $k_{\eta_2} = 0.25$, $\sigma = 0.001$, $z_\theta = 1$, $a = 0.0005$, $\omega = 0.5$ rad/h, $k = 0.01$	Fig. 11
	u_ϕ	$k_T = 2$, $k_{\eta_1} = 0.25$, $k_{\eta_2} = 0.25$, $\sigma = 0.001$, $z_\theta = 1$, $a = 0.0005$, $\omega = 0.5$ rad/h, $k = 0.01$	
SESC	$J_{T,sp}$	$\rho = 0.75$, $\chi = 2$, $\gamma = 0.6$, $\sigma = 0.6$, $T_s = 2$ h	Fig. 11
	u_ϕ	$\rho = 0.75$, $\chi = 2$, $\gamma = 0.6$, $\sigma = 0.6$, $T_s = 2$ h	

does not cause the convergence criteria to be exceeded. The final mean value is determined by averaging the objective function over the last 5-hour period of the scenario. The earliest instance for which J remains within the 2% threshold is used as the time taken for convergence.

6.1. Simulation environment

A sampling period of 60 seconds is used to ensure sufficient representation of the dynamics of the system. White Gaussian noise with a noise level of -10 dB is added to Q_s, and -50 dB is added to J_T and ψ to evaluate the performance of the ESCs subject to measurement noise. Furthermore, for all the simulations the ESCs are restricted to explore in a region that is defined by the grind curves, $J_T \in [0.20, 0.45]$ and $u_\phi \in [0.60, 0.75]$ by enforcing hard constraints on both J_T and u_ϕ.

6.2. Single plant output optimization

In single output optimization, only one plant output is optimized by the ESC and the other output is left uncontrolled. The results are shown in Figs. 11–14. The convergence results and tuning parameters used are summarized in Tables 4–11.

6.2.1. ESC perturbing a single variable (SISO)

In this section, either $J_{T,sp}$ or u_ϕ is individually manipulated to optimize Q_s or ψ. It is assumed that switch A or B, as shown in Fig. 10, is closed by an operator for the purposes of this section. This configuration is referred to as single-input-single-output (SISO) optimization in this paper. Switch A is closed initially up until such time as $J_{T,sp}$ does not change anymore, after which B is closed with A open. For throughput optimization (Fig. 11) the switchover from A to B happens at $t = 50$ hours, and for grind optimization (Fig. 12) at $t = 100$ hours. Since $J_{T,sp}$ and u_ϕ are not simultaneously perturbed, the ESCs do not need distinct tuning parameters between $J_{T,sp}$ or

Table 5: SISO throughput (Q_s) optimization results. $\overline{Q}_{s_1}$ indicates the average peak reached with J_T and $\overline{Q}_{s_2}$ indicates the average peak reached with u_ϕ.

Method	Average value	Convergence time	Results
PESC	$\overline{Q}_{s_1} = 120.3$ m^3/h	15.9 h	Fig. 11
	$\overline{Q}_{s_2} = 155.9$ m^3/h	14.0 h	
TESC	$\overline{Q}_{s_1} = 120.5$ m^3/h	18.5 h	Fig. 11
	$\overline{Q}_{s_2} = 154.3$ m^3/h	13.3 h	
SESC	$\overline{Q}_{s_1} = 120.3$ m^3/h	27.7 h	Fig. 11
	$\overline{Q}_{s_2} = 154.8$ m^3/h	3.9 h	

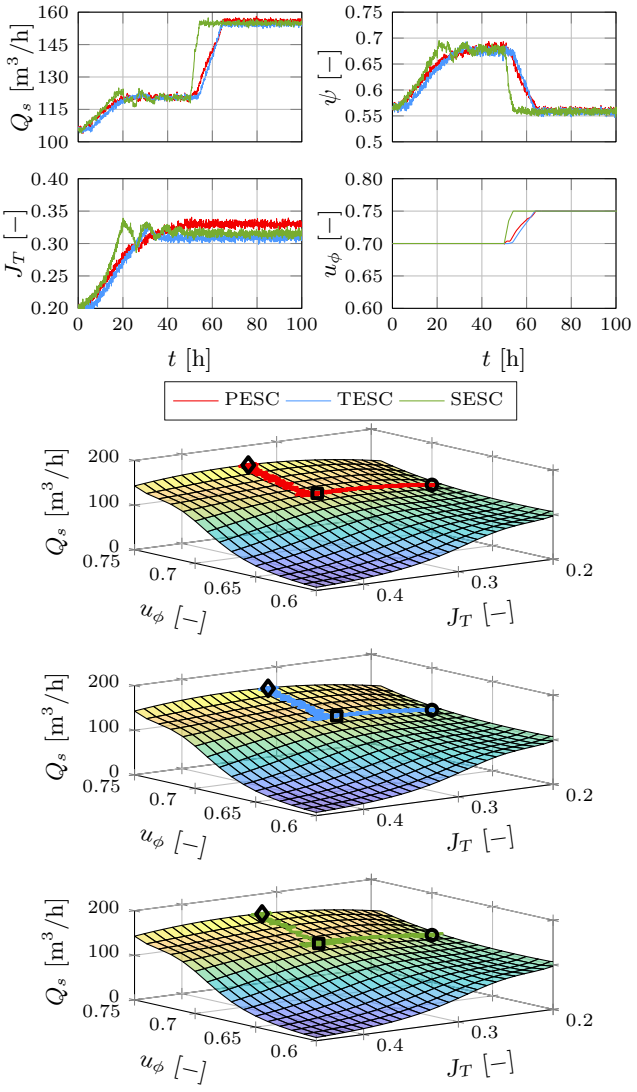

Fig. 11: Comparison of SISO throughput (Q_s) optimization with J_T for $t \leq 50$ hours and with u_ϕ for $t > 50$ hours. The initial conditions are indicated by ○, the switchover occurring at $t = 50$ h is indicated by □, and the final time conditions are indicated by ♢.

Table 6: SISO grind (ψ) ESC tuning parameters.

Method	Manipulated variable	Tuning parameter values	Results
PESC	$J_{T,sp}$	$k = 4000$, $a = 0.002$, $\omega_h = 1.8$ rad/h, $\omega = 2$ rad/h, $\omega_l = 0.1$ rad/h	Fig. 12
	u_ϕ	$k = 4000$, $a = 0.001$, $\omega_h = 1.6$ rad/h, $\omega = 2$ rad/h, $\omega_l = 0.05$ rad/h	
TESC	$J_{T,sp}$	$k_T = 3$, $k_{\eta_1} = 0.25$, $k_{\eta_2} = 0.25$, $\sigma = 1e-05$, $z_\theta = 1$, $a = 0.001$, $\omega = 1$ rad/h, $k = 0.01$	Fig. 12
	u_ϕ	$k_T = 3$, $k_{\eta_1} = 0.25$, $k_{\eta_2} = 0.25$, $\sigma = 1e-05$, $z_\theta = 1$, $a = 0.001$, $\omega = 1$ rad/h, $k = 0.01$	
SESC	$J_{T,sp}$	$\rho = 0.6$, $\chi = 2$, $\gamma = 0.4$, $\sigma = 0.6$, $T_s = 2$ h	Fig. 12
	u_ϕ	$\rho = 0.6$, $\chi = 2$, $\gamma = 0.4$, $\sigma = 0.6$, $T_s = 2$ h	

u_ϕ to distinguish their effects on the direction of the objective function. The results comparing the ESC methods are shown in Figs. 11–12.

For throughput (Q_s) optimization (Fig. 11), for $t <= 50$ hours the ESCs steer the process toward the optimum by manipulating $J_{T,sp}$. The ESCs then switch to manipulate u_ϕ for $t > 50$ hours and $J_{T,sp}$ is maintained at the current best operating point obtained by the ESCs. The final value reached for Q_s for each method varies based on the final value of $J_{T,sp}$ reached before switching from manipulating $J_{T,sp}$ to u_ϕ. Therefore, each method may reach different values of Q_s at the final conditions. All three ESC methods tend to follow the same trajectory in tracking the extremum for Q_s along J_T and then u_ϕ. SESC makes relatively large steps in comparison to PESC and TESC. However, the large steps cause the method to temporarily oscillate around the neighbourhood of the optimal J_T. TESC initially has a delay before it begins to converge and manipulate $J_{T,sp}$ or u_ϕ as seen in Fig. 11.

For grind (ψ) optimisation (Fig. 12), for $t <= 100$ hours the ESCs steer the process toward the optimum by manipulating $J_{T,sp}$. The ESCs then manipulate u_ϕ for $t > 100$ hours and $J_{T,sp}$ is maintained at the current best operating point obtained by the ESCs. The final value reached for ψ for each method varies based on the final value of $J_{T,sp}$ reached. The ESCs have a longer convergence time when optimizing ψ compared to Q_s when perturbing u_ϕ. Furthermore, as the grind approaches $\psi \to 0.8$ when the mill speed approaches $u_\phi \to 0.6$, the relationship between u_ϕ and ψ is relatively flat and the extracted gradient information is primarily due to the measurement noise. SESC converges relatively quickly to the ψ peak as it is robust to measurement noise. However, PESC and TESC take longer to converge, which can be attributed to the effects of noise as there is an insignificant gradient change between ψ and u_ϕ.

If u_ϕ is fixed, each ESC method converges to relatively

Table 7: SISO grind (ψ) optimization results. $\overline{\psi}_1$ indicates the average peak reached with J_T and $\overline{\psi}_2$ indicates the average peak reached with u_ϕ.

Method	Average value	Convergence time	Results
PESC	$\overline{\psi}_1 = 0.56$	11.1 h	Fig. 12
	$\overline{\psi}_2 = 0.77$	150.1 h	
TESC	$\overline{\psi}_1 = 0.56$	21.9 h	Fig. 12
	$\overline{\psi}_2 = 0.79$	97.1 h	
SESC	$\overline{\psi}_1 = 0.56$	5.5 h	Fig. 12
	$\overline{\psi}_2 = 0.81$	14.2 h	

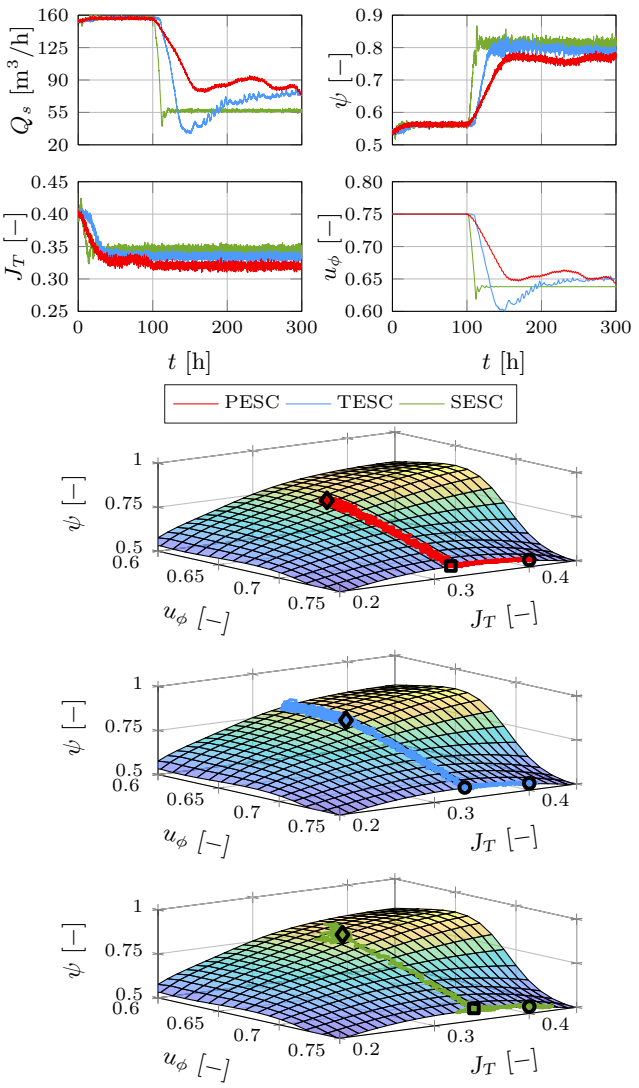

Fig. 12: Comparison of SISO grind (ψ) optimization with J_T for $t \leq 100$ hours and with u_ϕ for $t > 100$ hours. The initial conditions are indicated by ○, the switchover occurring at $t = 100$ h is indicated by □, and the final time conditions are indicated by ◇.

Table 8: MISO throughput (Q_s) ESC tuning parameters.

Method	Manipulated variable	Tuning parameter values	Results
PESC	$J_{T,sp}$	$k = 20$, $a = 0.002$, $\omega_h = 1.5$ rad/h, $\omega = 1.6$ rad/h, $\omega_l = 0.05$ rad/h	Fig. 13
	u_ϕ	$k = 20$, $a = 0.002$, $\omega_h = 1.8$ rad/h, $\omega = 2$ rad/h, $\omega_l = 0.05$ rad/h	
TESC	$J_{T,sp}$	$k_T = 1$, $k_{\eta_1} = 0.25$, $k_{\eta_2} = 0.25$, $\sigma = 0.001$, $z_\theta = 1$, $a = 0.0001$, $\omega = 0.5$ rad/h, $k = 0.01$	Fig. 13
	u_ϕ	$k_T = 2$, $k_{\eta_1} = 0.5$, $k_{\eta_2} = 0.5$, $\sigma = 0.001$, $z_\theta = 1$, $a = 0.0001$, $\omega = 0.5$ rad/h, $k = 0.02$	
SESC	$J_{T,sp}$	$\rho = 0.75$, $\chi = 2$, $\gamma = 0.6$, $\sigma = 0.1$, $T_s = 2$ h	Fig. 13
	u_ϕ	$\rho = 0.75$, $\chi = 2$, $\gamma = 0.6$, $\sigma = 0.1$, $T_s = 2$ h	

similar operating conditions to optimize Q_s or ψ as shown in Tables 5 and 7.

6.2.2. ESC with perturbing multiple variables (MISO)

In this section, $J_{T,sp}$ and u_ϕ are manipulated together (both switches A and B are closed in Fig. 10) to optimize either Q_s or ψ. This configuration is referred to as multiple-input-single-output (MISO) optimization in this paper.

For throughput (Q_s) optimization (Fig. 13), all three ESCs behave relatively similarly and u_ϕ quickly converges to the maximum mill speed compared to J_T. There is a strong positive correlation between Q_s and u_ϕ, where the throughput increases as the mill speed increases. However, the optimal J_T lies between $J_T \in [0.20, 0.45]$ for different values of u_ϕ. Therefore, J_T takes longer to settle within the neighbourhood of its optimal value.

For grind (ψ) optimization (Fig. 14), PESC converges to a different operating condition as compared to TESC and PESC. This is due to the difference in the optimization gains chosen for the tuning parameters for PESC (Table 10). Due to the faster adaptation of u_ϕ with TESC and SESC, both of these ESC methods reach the limit of u_ϕ and search along J_T to find the ψ peak. As the ESCs converge to $u_\phi \to 0.60$, the model response of ψ at higher values of J_T begins to flatten. The influence of noise is sufficient to prevent the ESCs from exploring further due to the insignificant increase in the measured ψ along the J_T axis. However, with PESC, the ESC adapts J_T toward its upper limit compared to TESC and SESC, which both adapted u_ϕ toward the lower limit. Therefore, u_ϕ is used to steer the plant toward the ψ peak once J_T reached its upper limit. In all cases, the ESCs steered the process toward a higher J_T and lower u_ϕ, where the ψ peak is likely to be located.

Careful consideration has to be given to the parameters associated with the optimization speed used for each perturbed input. If the tuning parameters are poorly chosen for either of the inputs, the effects of the perturbed input will be negligible on the output relative to the other perturbed input. As a result, the ESC is likely to adapt one of the inputs over the other. For example, similar optimization gain values are used for PESC in the results

Table 9: MISO throughput (Q_s) optimization results.

Method	Average value	Convergence time	Results
PESC	$\overline{Q}_s = 153.0$ m^3/h	85.6 h	Fig. 13
TESC	$\overline{Q}_s = 153.1$ m^3/h	58.6 h	Fig. 13
SESC	$\overline{Q}_s = 153.2$ m^3/h	100 h	Fig. 13

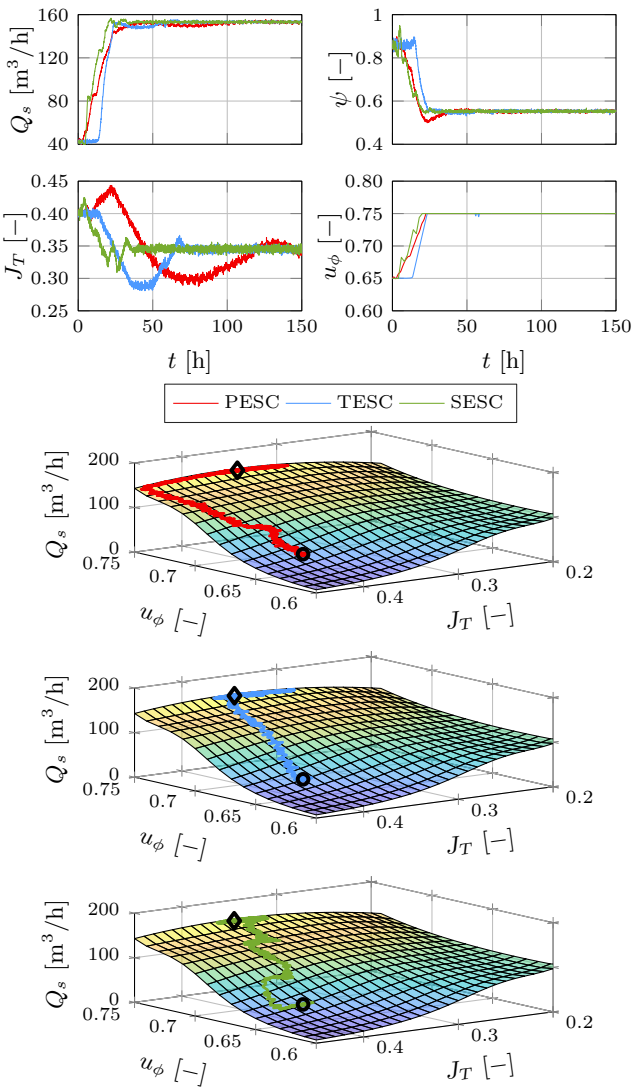

Fig. 13: Comparison of MISO throughput (Q_s) optimization with both J_T and u_ϕ. The initial conditions are indicated by ○ and the final time conditions are indicated by ♢.

Table 10: MISO grind (ψ) ESC tuning parameters.

Method	Manipulated variable	Tuning parameter values	Results
PESC	$J_{T,sp}$	$k = 2000$, $a = 0.002$, $\omega_h = 1.5$ rad/h, $\omega = 1.6$ rad/h, $\omega_l = 0.05$ rad/h	Fig. 14
	u_ϕ	$k = 500$, $a = 0.002$, $\omega_h = 1.8$ rad/h, $\omega = 2$ rad/h, $\omega_l = 0.05$ rad/h	
TESC	$J_{T,sp}$	$k_T = 0.75$, $k_{\eta_1} = 0.75$, $k_{\eta_2} = 0.75$, $\sigma = 1e-05$, $z_\theta = 1$, $a = 0.001$, $\omega = 0.5$ rad/h, $k = 0.01$	Fig. 14
	u_ϕ	$k_T = 1$, $k_{\eta_1} = 0.25$, $k_{\eta_2} = 0.25$, $\sigma = 1e-05$, $z_\theta = 1$, $a = 0.001$, $\omega = 1$ rad/h, $k = 0.01$	
SESC	$J_{T,sp}$	$\rho = 0.9$, $\chi = 2$, $\gamma = 0.5$, $\sigma = 0.5$, $T_s = 4$ h	Fig. 14
	u_ϕ	$\rho = 0.9$, $\chi = 2$, $\gamma = 0.5$, $\sigma = 0.5$, $T_s = 4$ h	

shown in Fig. 13. However, PESC tends to adapt u_ϕ faster compared to J_T. The effects of this are not crucial for optimizing the process if there is only a global extremum, but if there are multiple extremums the process could converge toward a local extremum and operate at sub-optimal operating conditions. The results in Figs. 13 and 14 emphasize that the ESCs do converge toward the neighbourhood of an unknown peak. However, the initial conditions and the tuning parameters are important to consider when applying ESC to optimize the grinding mill performance as both these factors influence the convergence trajectory of the ESC.

6.3. Multiple plant output optimization

The strategies mentioned thus far demonstrate that extremum seeking can operate the grinding mill at an extremum for either Q_s or ψ. However, optimizing for one of the outputs leaves the other output at a suboptimum operating point.

From a practical perspective, optimizing ψ at the cost of significantly reducing Q_s or vice-versa may not be ideal in meeting operational objectives. Depending on the market value of the valuable minerals produced, it could also be beneficial to maximize ψ while processing a sufficient amount of ore material (Q_s). The inverse relationship that exists between Q_s and ψ indicates that a balance between both outputs has to be considered to maximize profits [47]. This section addresses the ways in which ESC can be applied to avoid the observed decreased performance shown in the single output optimization cases. In multiple output optimization, both outputs are considered when optimizing the mill performance with ESC. The results are shown in Figs. 16–20. The convergence results and tuning parameters used are summarized in Tables 12–17.

Table 11: MISO grind (ψ) optimization results.

Method	Average value	Convergence time	Results
PESC	$\overline{\psi} = 0.84$	137.87 h	Fig. 14
TESC	$\overline{\psi} = 0.80$	82.9 h	Fig. 14
SESC	$\overline{\psi} = 0.81$	106.9 h	Fig. 14

6.3.1. ESC with a weighted objective function

In this section, an optimization strategy is proposed to optimize the mill performance with the use of a weighted objective function using the control configuration shown in Fig. 10 with switches A and B closed. Both Q_s and

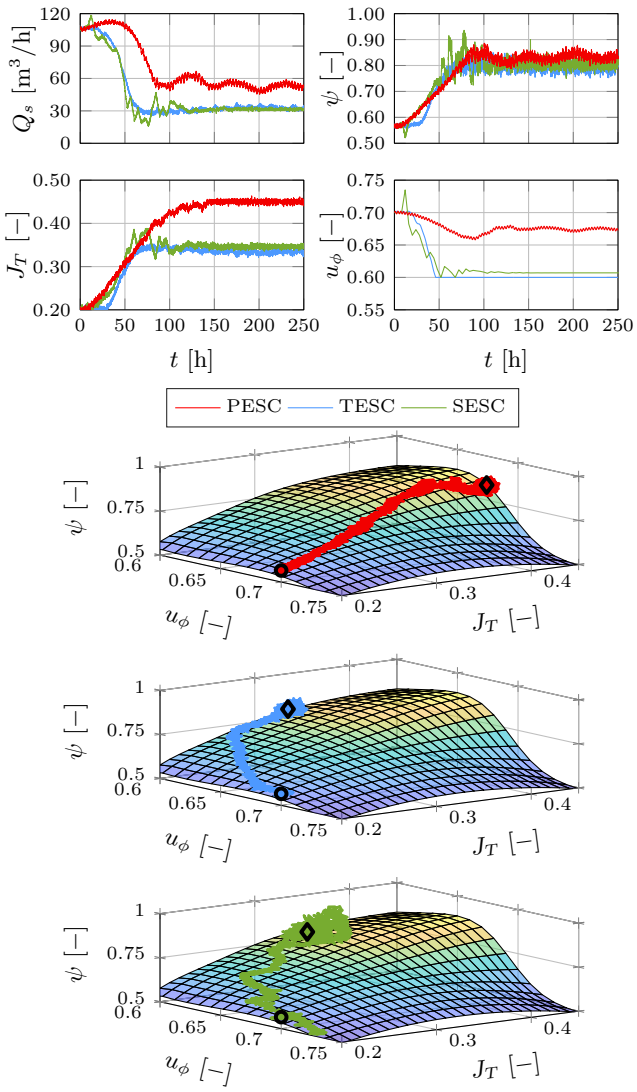

Fig. 14: Comparison of MISO grind (ψ) optimization with both J_T and u_ϕ. The initial conditions are indicated by ○ and the final time conditions are indicated by ♢.

Table 12: Single input, weighted objective PESC tuning parameters.

Method	Manipulated variable	Tuning parameter values	Results
PESC	$J_{T,sp}$	$k = 2000$, $a = 0.001$, $\omega_h = 1.2$ rad/h, $\omega = 1.4$ rad/h, $\omega_l = 0.05$ rad/h	Fig. 16

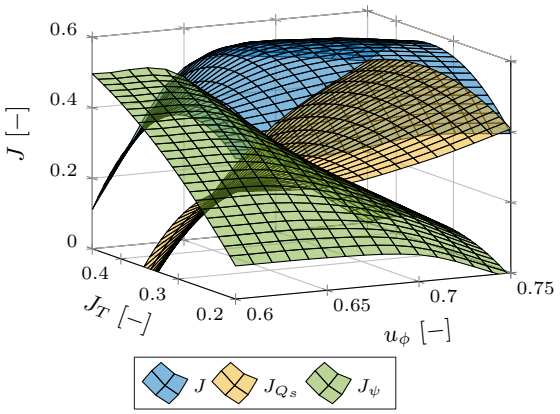

Fig. 15: Contribution of J_{Q_s} and J_ψ to J with $\lambda = 0.5$.

ψ are scaled using min-max normalization to ensure that both outputs contribute relatively equally in magnitude across the range of J_T and u_ϕ. The objective function is formulated as,

$$J(Q_s,\ \psi) = \lambda J_{Q_s} + (1-\lambda)J_\psi, \tag{22a}$$

$$J_{Q_s} = \frac{Q_s - Q_{s,min}}{Q_{s,max} - Q_{s,min}}, \tag{22b}$$

$$J_\psi = \frac{\psi - \psi_{min}}{\psi_{max} - \psi_{min}}, \tag{22c}$$

where $Q_{s,min} = 0$ m^3/h, $Q_{s,max} = 158$ m^3/h, $\psi_{min} = 0.5$, and $\psi_{max} = 0.93$, which are chosen based on the theoretically smallest and largest values obtained from the grind curves (Fig. 4). These values could also be chosen based on the design specifications of the grinding mill. The weighting factor is denoted by λ and is used to adjust the contribution of Q_s or ψ to the objective function, J. To illustrate the contribution of J_{Q_s} or J_ψ for an equal weighting of $\lambda = 0.5$, the 3-D surface of the objective function is shown in Fig. 15.

The results of the weighted objective function optimization strategy are shown only for PESC in Fig. 16, where the ESC perturbs only a single variable, $J_{T,sp}$, to maximize the weighted objective function. The advantage of employing a weighted objective function is that only a single variable is necessary for the ESC to achieve a balance between Q_s and ψ and meet operational objectives.

Table 13: Single input, weighted objective PESC optimization results.

λ	Average value	Convergence time	Results
0.4	$\overline{Q}_s = 57.09$ m^3/h $\overline{\psi} = 0.83$ $\overline{J} = 0.60$	112.6 h	Fig. 16
0.5	$\overline{Q}_s = 75.92$ m^3/h $\overline{\psi} = 0.78$ $\overline{J} = 0.57$	68.4 h	Fig. 16
0.6	$\overline{Q}_s = 85.3$ m^3/h $\overline{\psi} = 0.75$ $\overline{J} = 0.56$	55.0 h	Fig. 16

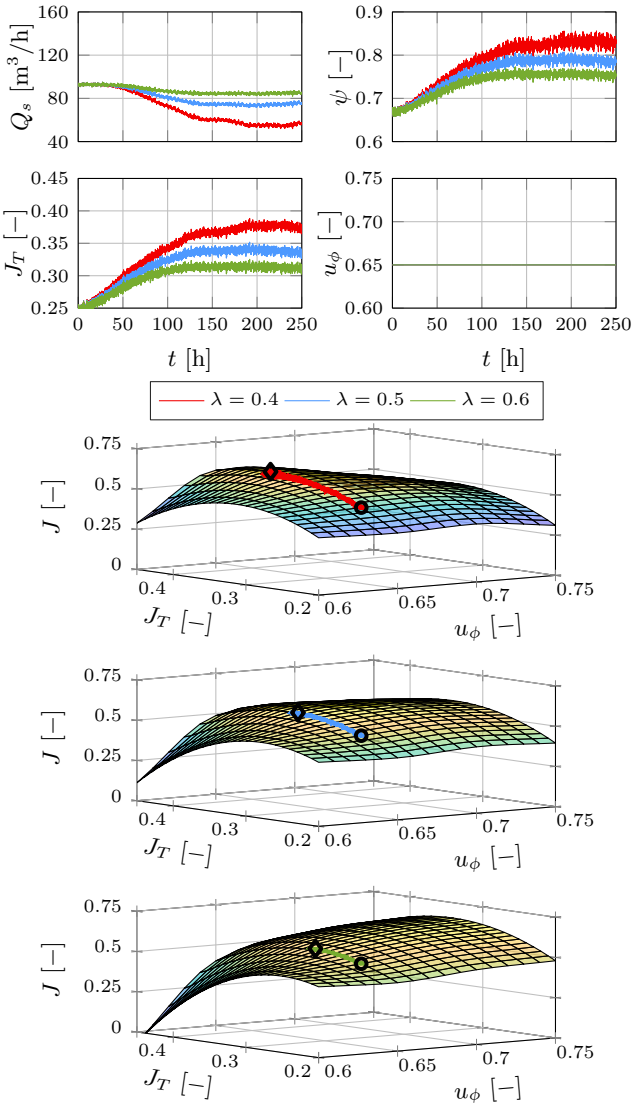

Fig. 16: Single input, weighted objective PESC optimization. The 3-D surface maps of J vary as the value of λ is adjusted. The initial conditions are indicated by ○ and the final time conditions are indicated by ◇.

Table 14: MIMO throughput (Q_s) ESC tuning parameters.

Method	Manipulated variable	Tuning parameter values	Results
PESC	$J_{T,sp}$	$k = 20$, $a = 0.002$, $\omega_h = 1.8$ rad/h, $\omega = 2$ rad/h, $\omega_l = 0.1$ rad/h	Fig. 18
TESC	$J_{T,sp}$	$k_T = 2$, $k_{\eta_1} = 0.25$, $k_{\eta_2} = 0.25$, $\sigma = 0.001$, $z_\theta = 1$, $a = 0.0005$, $\omega = 0.5$ rad/h, $k = 0.01$	Fig. 18
SESC	$J_{T,sp}$	$\rho = 0.8$, $\chi = 2$, $\gamma = 0.5$, $\sigma = 0.5$, $T_s = 2$ h	Fig. 18

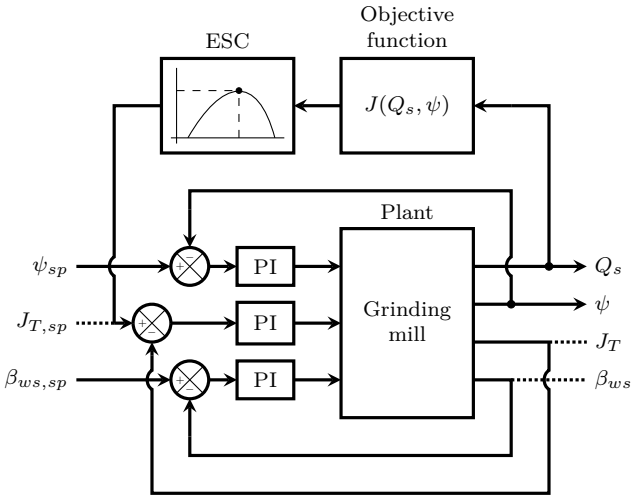

Fig. 17: Block diagram of the grinding mill with the throughput (Q_s) optimized with ESC and the grind (ψ) is regulated at setpoint.

Using the weighted objective function to optimize a process with multiple outputs would be beneficial if there are fewer inputs than there are outputs. This would be the case if, for example, the grinding mill is not equipped with a variable speed drive to vary u_ϕ. In this case, J_T is used to optimize for both Q_s and ψ, but with the inverse relationship between the outputs, the plant operator would have to consider a trade-off between Q_s and ψ.

Employing the weighted objective function would mean that the performance of Q_s or ψ does not drastically decrease as is seen in the single output optimization results. Instead, λ is used as a parameter to reach an acceptable Q_s or ψ, and the ESC would track the extremum of the objective function. However, in order to effectively balance between Q_s and ψ, some prior knowledge of the unknown grind curves would be necessary to choose a suitable value for λ. For example, the plant operator cannot explicitly choose the value of Q_s or ψ that the grinding mill will operate at by choosing λ. It is also not a linear relationship as can be seen in Fig. 16 and Table 13. The measured Q_s and ψ do not scale proportionally with λ. Further, the grind curves are time-varying due to varying feed ore characteristics, which could affect the contribution of J_{Q_s} and J_ψ over time.

Table 15: MIMO throughput (Q_s) optimization results.

Method	Average value	Convergence time	Results
PESC	$\overline{Q}_s = 113.7$ m^3/h $\overline{\psi} = 0.70$	41.9 h	Fig. 18
TESC	$\overline{Q}_s = 115.0$ m^3/h $\overline{\psi} = 0.70$	52.3 h	Fig. 18
SESC	$\overline{Q}_s = 114.7$ m^3/h $\overline{\psi} = 0.70$	39.7 h	Fig. 18

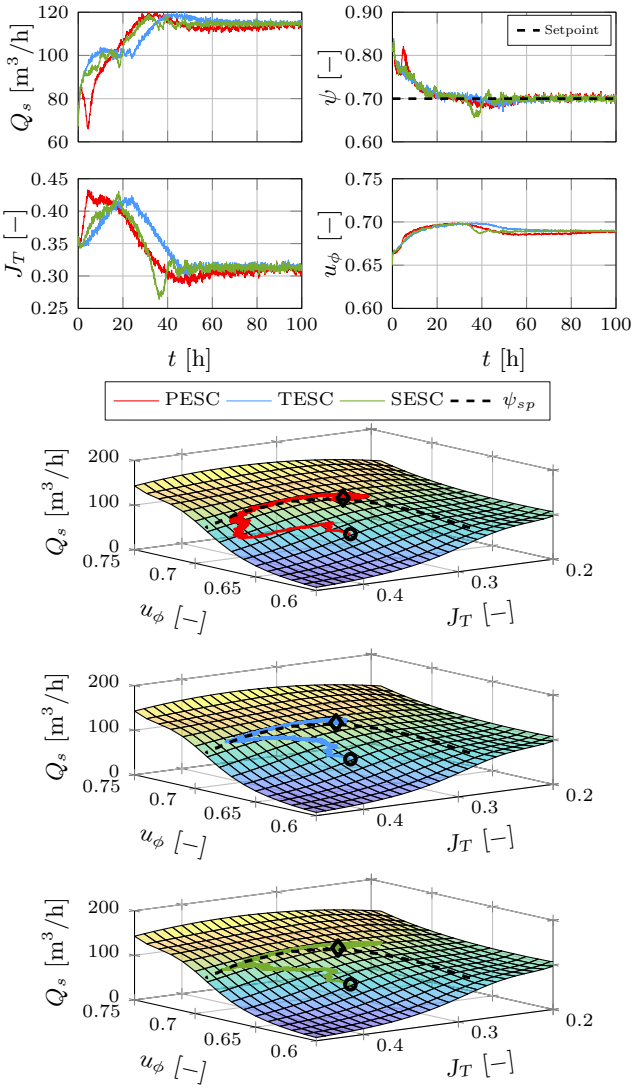

Fig. 18: Comparison of MIMO throughput (Q_s) optimization with J_T and ψ is controlled at setpoint with u_ϕ. The black dashed line on the 3-D surface maps indicates the operating conditions (J_T and u_ϕ) where $\psi_{sp} = 0.7$. The initial conditions are indicated by ○ and the final time conditions are indicated by ◇.

Table 16: MIMO grind (ψ) ESC tuning parameters.

Method	Manipulated variable	Tuning parameter values	Results
PESC	$J_{T,sp}$	$k = 4000$, $a = 0.002$, $\omega_h = 1.8$ rad/h, $\omega = 2$ rad/h, $\omega_l = 0.1$ rad/h	Fig. 20
TESC	$J_{T,sp}$	$k_T = 3$, $k_{\eta_1} = 0.25$, $k_{\eta_2} = 0.25$, $\sigma = 1e-05$, $z_\theta = 1$, $a = 0.0001$, $\omega = 1$ rad/h, $k = 0.01$	Fig. 20
SESC	$J_{T,sp}$	$\rho = 0.6$, $\chi = 2$, $\gamma = 0.5$, $\sigma = 0.5$, $T_s = 2$ h	Fig. 20

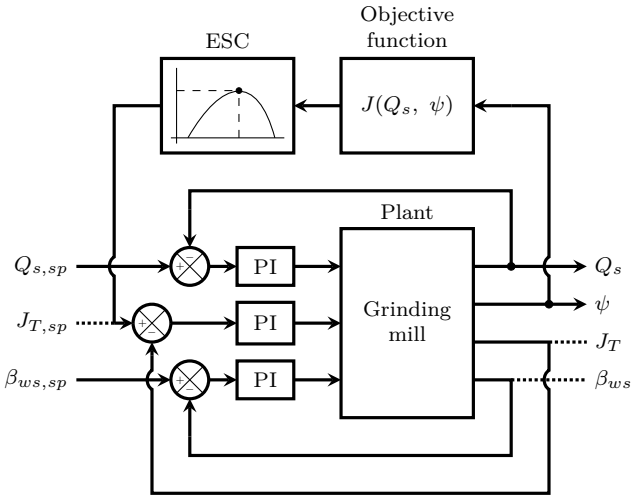

Fig. 19: Block diagram of the grinding mill with the grind (ψ) optimized with ESC and the throughput (Q_s) is regulated at setpoint.

6.3.2. ESC with paired control

Paired multi-input-multi-output (MIMO) control ensures that the operational objectives are satisfied while optimizing the process by utilizing the mill variables J_T and u_ϕ to optimize Q_s or ψ. The strategy pairs an output to be optimized (Q_s or ψ) with one of the manipulated variables ($J_{T,sp}$ or u_ϕ) to the ESC, while the other output is paired to the remaining manipulated variable and controlled to setpoint by a regulatory controller as shown in Figs. 17 and 19. This strategy is useful when considering the environmental issues associated with the comminution stage. From an environmental perspective, there is a significant amount of valuable minerals that could be lost to the tailings in the separation process if the grind quality is poor. Most commonly, the mill is operated to maximize Q_s while achieving the minimum acceptable ψ. Therefore, to reduce the waste of valuable minerals lost to waste or if the market demand leans toward a high-grade concentrate, it would be beneficial to achieve an increased ψ as opposed to maximizing Q_s. The paired control strategy enables the processing plant to satisfy operational objectives for either Q_s or ψ while maximizing the net economic benefit.

Table 17: MIMO grind (ψ) optimization results.

Method	Average value	Convergence time	Results
PESC	$\overline{\psi} = 0.74$ $\overline{Q}_s = 99.88$ m^3/h	54.2 h	Fig. 20
TESC	$\overline{\psi} = 0.75$ $\overline{Q}_s = 99.97$ m^3/h	31.8 h	Fig. 20
SESC	$\overline{\psi} = 0.75$ $\overline{Q}_s = 99.94$ m^3/h	16.6 h	Fig. 20

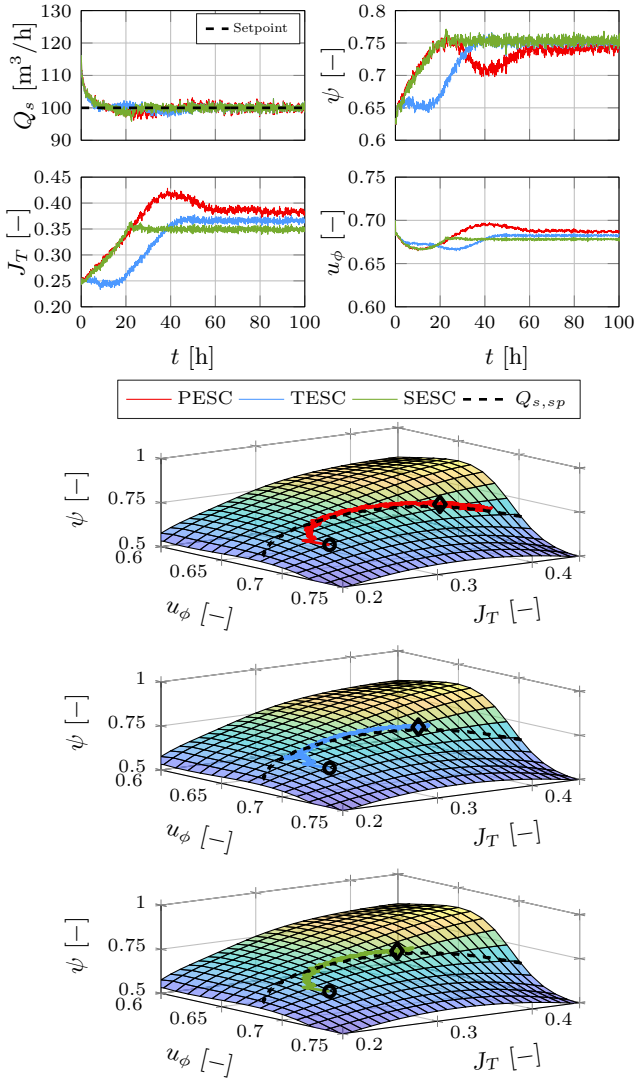

Fig. 20: Comparison of MIMO grind (ψ) optimization with J_T and Q_s is controlled at setpoint with u_ϕ. The black dashed line on the 3-D surface maps indicates the operating conditions (J_T and u_ϕ) where $Q_{s,sp} = 100$ m^3/h. The initial conditions are indicated by ○ and the final time conditions are indicated by ◇.

The results for both scenarios where ψ or Q_s is regulated at setpoint is shown in Figs. 18 and 20, respectively. In both cases, the regulatory controllers and the ESCs operate together without significantly hindering each other's performance. The regulatory controllers are able to drive the outputs to their setpoints, while the ESCs track the extremum along the operating conditions given by the setpoints.

6.4. Choosing an ESC

Choosing an ESC to optimize the grinding mill performance is based on several factors such as speed of convergence, accuracy, and ease of tuning. PESC is simple to tune. However, the convergence performance of PESC is limited to the dynamics of the plant. Furthermore, the dither signal amplitude should be large enough to overpower the effects of noise, but it should also not be too large such that it causes excessive variations in the measured output.

TESC is favourable as a dither-based extremum seeking method due to the smaller dither signal that can be used. For most of the simulated results, the amplitude of the dither signal used for TESC was an order of magnitude smaller than the amplitude for the dither signal used in PESC. Furthermore, TESC does not have tuning parameters that are necessarily limited to the dynamics of the process, but it does have the most tuning parameters (8) when compared to PESC (5) and SESC (4). The TESC method can be more difficult to tune as it has more parameters and requires a better fundamental understanding of the ESC method than the PESC and SESC methods.

SESC is favourable as a dither-free extremum seeking method due to the lack of perturbations. However, the lack of gradient information indicates that the controller will not continue to operate near optimal conditions if the extremum is time-varying. The SESC method does also require basic knowledge of the plant dynamics to ensure a sufficient amount of time for the plant to settle. If the settling time chosen is too long, the plant will unnecessarily operate sub-optimally until it reaches the extremum. However, if the settling time is too short, the method will not be able to effectively steer the plant toward the extremum. Furthermore, SESC is robust to measurement noise since the method operates on the functional value of the objective function rather than the gradient information. Additionally, if the SESC tuning parameters are not conservatively chosen, it can cause the ESC to require large step changes that push the system close to or beyond the acceptable operating boundaries.

7. Conclusion

This paper investigates several optimization strategies to improve grinding mill performance by manipulating the mill load or speed. The single output optimization results show that ESC is useful in steering the process towards an extremum for a single output. However, this results in poor performance for the other outputs that are not optimized. The weighted objective function and the paired control strategies show that ESC can be useful to not only steer the process toward an optimum, but also satisfy the operational objectives for a grinding mill.

Although the grind curves are not time-varying in the simulated results, they are time-varying in practice due to feed ore variations. ESCs are beneficial as they can automatically and continuously track extremums and maintain process performance near optimal operating conditions. However, this is only achieved through gradient-based methods (PESC and TESC) that can adapt based on the changes measured in the objective function. SESC is only able to track an extremum for the initial period until it converges, after which the method maintains its current operating conditions and does not adjust them accordingly in the event of disturbances. In that case, the operating conditions are no longer optimal and the SESC needs to be reinitialized by an operator.

The simulation results given in this paper show that the ESCs have relatively long convergence times. This is acceptable if the feed ore characteristics do not frequently change. The convergence times depend on a number of factors, including the initial conditions chosen and the dynamics of the process in question. A plant operator can reduce the convergence time by choosing a good initial set of operating conditions based on prior knowledge. The focus of this paper was however not on the convergence times of the ESCs, but rather on their ability to steer the process toward an unknown optimum from different initial conditions.

Acknowledgement

This work is based on the research supported by the National Research Foundation of South Africa (IRC grant number 130569).

References

[1] B. A. Wills, J. A. Finch, Wills' Mineral Processing Technology: An Introduction to the Practical Aspects of Ore Treatment and Mineral Recovery, 8th Edition, Butterworth-Heinemann, Oxford, 2015.

[2] T. J. Napier-Munn, S. Morrell, R. D. Morrison, T. Kojovic, Mineral Communition Circuits: Their Operation and Optimisation, 3rd Edition, Julius Kruttschnitt Mineral Research Centre, Isles Road, Indooroopilly, Queensland 4068, Australia, 2005.

[3] A. Gupta, D. S. Yan, Mineral Processing Design and Operation: An Introduction, 1st Edition, Elsevier, Oxford, 2016.

[4] J. D. le Roux, I. K. Craig, Plant-wide control framework for a grinding mill circuit, Industrial and Engineering Chemistry Research 58 (2019) 11585–11600.

[5] D. Wei, I. K. Craig, Grinding mill circuits - A survey of control and economic concerns, International Journal of Mineral Processing 90 (2009) 56–66.

[6] M. G. Maritz, J. D. le Roux, I. K. Craig, Feed size distribution feedforward control for a grinding mill circuit, IFAC-PapersOnLine 52 (2019) 7–12.

[7] J. Tessier, C. Duchesne, G. Bartolacci, A machine vision approach to on-line estimation of run-of-mine ore composition on conveyor belts, Minerals Engineering (2007) 1129–1144.
[8] S. Morrell, W. M. Finch, T. Kojovic, H. Delboni Jr., Modelling and simulation of large diameter autogeneous and semi-autogeneous mills, International Journal of Mineral Processing 44-45 (1996) 289–300.
[9] P. Zhou, S. Lu, M. Yuan, T. Chai, Survey on higher-level advanced control for grinding circuits operation, Powder Technology 288 (2016) 324–338.
[10] D. Hodouin, Methods for automatic control, observation, and optimization in mineral processing plants, Journal of Process Control 21 (2011) 211–225.
[11] L. E. Olivier, I. K. Craig, A survey on the degree of automation in the mineral processing industry, 2017 IEEE AFRICON (2017) 404–409.
[12] M. Benosman, Learning-based Adaptive Control: An Extremum Seeking Approach - Theory and Applications, 1st Edition, Butterworth-Heinemann, Oxford, 2016.
[13] K. Åström, B. Wittenmark, Adaptive Control, 2nd Edition, Dover Books on Electrical Engineering, Dover Publications, 2013.
[14] M. Krstić, H. Wang, Design and stability analysis of extremum seeking feedback for general nonlinear systems, Proceedings of the 36th IEEE Conference on Decision and Control 2 (1997) 1743–1748.
[15] S. Korovin, V. Utkin, Using sliding modes in static optimization and nonlinear programming, Automatica 10 (5) (1974) 525–532.
[16] Y. Pan, Ümit Özgüner, T. Acarman, Stability and performance improvement of extremum seeking control with sliding mode, International Journal of Control 76 (9-10) (2003) 968–985.
[17] L. Fu, Ümit Özgüner, Extremum seeking with sliding mode gradient estimation and asymptotic regulation for a class of nonlinear systems, Automatica 47 (12) (2011) 2595–2603.
[18] W. H. Moase, C. Manzie, M. J. Brear, Newton-like extremum-seeking part I: Theory, Proceedings of the 48th IEEE Conference on Decision and Control (CDC) held jointly with 2009 28th Chinese Control Conference (2009) 3839–3844.
[19] A. Ghaffari, M. Krstić, D. Nešić, Multivariable Newton-based extremum seeking, Automatica 48 (8) (2012) 1759–1767.
[20] C. Zhang, R. Ordóñez, Extremum-seeking Control and Applications: A Numerical Optimization-Based Approach, 1st Edition, Springer-Verlag London, London, 2012.
[21] M. Guay, D. Dochain, A time-varying extremum-seeking control approach, Automatica 51 (2015) 356–363.
[22] M. Guay, D. Dochain, A proportional-integral extremum-seeking controller design technique, Automatica 77 (2017) 61–67.
[23] B. Hunnekens, M. Haring, N. van de Wouw, H. Nijmeijer, A dither-free extremum-seeking control approach using 1st-order least-squares fits for gradient estimation, 53rd IEEE Conference on Decision and Control (2014) 2679–2684.
[24] M. Chioua, B. Srinivasan, M. Guay, M. Perrier, Performance improvement of extremum seeking control using recursive least square estimation with forgetting factor, IFAC-PapersOnLine 49 (7) (2016) 424–429.
[25] X. Lu, M. Krstić, T. Chai, J. Fu, Hardware-in-the-loop multi-objective extremum-seeking control of mineral grinding, IEEE Transactions on Control Systems Technology 29 (2021) 961–971.
[26] O. G. Pauw, R. P. King, K. C. Garner, P. C. van Aswegen, The control of pebble mills at Buffelsfontein Gold Mine by use of a multivariable peak-seeking controller, Journal of the Southern African Institute of Mining and Metallurgy (1985) 89–96.
[27] I. K. Craig, D. G. Hulbert, G. Metzner, S. P. Moult, Optimized multivariable control of an industrial run-of-mine milling circuit, Journal of the Southern African Institute of Mining and Metallurgy 92 (1992) 169–176.
[28] M. S. Powell, S. Morrell, S. Latchireddi, Developments in the understanding of South African style SAG mills, Minerals Engineering 14 (2001) 1143–1153.
[29] A. P. van der Westhuizen, M. S. Powell, Milling curves as a tool for characterising SAG mill performance, in: Proceedings of the International Conference on Autogenous and Semi-Autogenous Grinding Technology, Vancouver, B.C., Canada, 2006, pp. 217–232.
[30] M. S. Powell, A. P. van der Westhuizen, A. N. Mainza, Applying grindcurves to mill operation and optimisation, Minerals Engineering 22 (2009) 625–632.
[31] C. Steyn, C. Sandrock, Benefits of optimisation and model predictive control on a fully autogenous mill with variable speed, Minerals Engineering 53 (2013) 113–123.
[32] A. Cortinovis, M. Mercangöz, T. Mathur, J. Poland, M. Blaumann, Nonlinear coal mill modeling and its application to model predictive control, Control Engineering Practice 21 (2013) 308–320.
[33] J. Le Roux, R. Padhi, I. K. Craig, Optimal control of grinding mill circuit using model predictive static programming: A new nonlinear MPC paradigm, Journal of Process Control 24 (2014) 29–40.
[34] J. D. le Roux, L. E. Olivier, M. A. Naidoo, I. K. Craig, Throughput and product quality control for a grinding mill circuit using non-linear MPC, Journal of Process Control 42 (2016) 35–50.
[35] S. Botha, J. D. le Roux, I. K. Craig, Hybrid non-linear model predictive control of a run-of-mine ore grinding mill circuit, Minerals Engineering 123 (2018) 49–62.
[36] S. C. Bouffard, Benefits of process control systems in mineral processing grinding circuits, Minerals Engineering 79 (2015) 139–142.
[37] L. A. Cramer, What is your PGM concentrate worth?, in: Third International Platinum Conference 'Platinum in Transformation', The Southern African Institute of Mining and Metallurgy, 2008, pp. 387–394.
[38] R. Edwards, A. Vien, R. Perry, Strategies for the instrumentation and control of grinding circuits, Mineral Processing Plant Design, Practice, and Control (2002) 2130–2151.
[39] T. Viklund, J. Albertsson, J. Burstedt, M. Isaksson, J. Söderlund, Evolution of AG mill control system at Boliden Mineral AB, Proceedings of the International Conference on Autogenous and Semi-Autogenous Grinding Technology (2006) 311–325.
[40] J. D. le Roux, I. K. Craig, D. G. Hulbert, A. L. Hinde, Analysis and validation of a run-of-mine ore grinding mill circuit model, Minerals Engineering 43-44 (2013) 121–134.
[41] J. D. le Roux, A. Steinboeck, A. Kugi, I. K. Craig, Steady-state and dynamic simulation of a grinding mill using grind curves, Minerals Engineering 152, 106208.
[42] D. Nešić, Y. Tan, I. Mareels, On the Choice of Dither in Extremum Seeking Systems: a Case Study, Proceedings of the 45th IEEE Conference on Decision and Control 44 (2006) 2789–2794.
[43] M. Guay, E. Moshkar, D. Dochain, A constrained extremum-seeking control approach, International Journal of Robust and Nonlinear Control 25 (2015) 3132–3153.
[44] J. A. Nelder, R. Mead, A simplex method for function minimization, Computer Journal 7 (1965) 308–313.
[45] J. Lagarias, J. Reeds, M. Wright, P. Wright, Convergence properties of the Nelder–Mead simplex method in low dimensions, SIAM Journal on Optimization 9 (1998) 112–147.
[46] Q. Xiong, A. Jutan, Continuous optimization using a dynamic simplex method, Chemical Engineering Science 56 (2003) 3817–3828.
[47] M. Bauer, I. K. Craig, Economic assessment of advanced process control – A survey and framework, Journal of Process Control (2008) 2–18.